Quantum Dynamical Calculation of Bound Rovibrational States of HO2 up to Largest Possible Total Angular Momentum, J <= 130

ARTICLE *in* THE JOURNAL OF PHYSICAL CHEMISTRY A · MAY 2013

Impact Factor: 2.69 · DOI: 10.1021/jp401154m · Source: PubMed

3 AUTHORS:

Corey Petty
Instituto Tecnologico de Aeronautica
3 PUBLICATIONS **9** CITATIONS
SEE PROFILE

Wenwu Chen
Lanzhou University
42 PUBLICATIONS **366** CITATIONS
SEE PROFILE

Bill Poirier
Texas Tech University
76 PUBLICATIONS **1,176** CITATIONS
SEE PROFILE

THE JOURNAL OF PHYSICAL CHEMISTRY A

Article

pubs.acs.org/JPCA

Quantum Dynamical Calculation of Bound Rovibrational States of HO_2 up to Largest Possible Total Angular Momentum, $J \leq 130$

Corey Petty, Wenwu Chen, and Bill Poirier*

Department of Chemistry and Biochemistry, and Department of Physics, Texas Tech University, Box 41061, Lubbock, Texas 79409-1061, United States

Supporting Information

ABSTRACT: In a previous article [*J. Theor. Comput. Chem.* **2010**, *9*, 435], all rovibrational bound states of HO_2 were systematically computed, for all total angular momentum values $J = 0-10$. In this article, the high-J rovibrational states are computed for every multiple-of-ten J value up to $J = 130$, which is the point where the centrifugal barrier obliterates the potential well, and bound states no longer exist. The results are used to assess the importance of Coriolis coupling in this floppy system and to evaluate two different J-shifting schemes. Though not effective for multiply vibrationally excited bound states, vibrational-state-dependent J-shifting obtains modestly accurate predictions for the lowest-lying energies [*J. Phys. Chem. A* **2006**, *110*, 3246]. However, much better performance is obtained—especially for large J values, and despite substantial Coriolis coupling—using a second, rotational-state-dependent J-shifting scheme [*J. Chem. Phys.* **1998**, *108*, 5216], for which the rotational constants themselves depend on J and K. The latter formalism also yields important dynamical insight into the structure of the strongly Coriolis-coupled eigenstate wave functions. The calculations were performed using ***ScalIT***, a suite of codes enabling quantum dynamics calculations on massively parallel computing architectures.

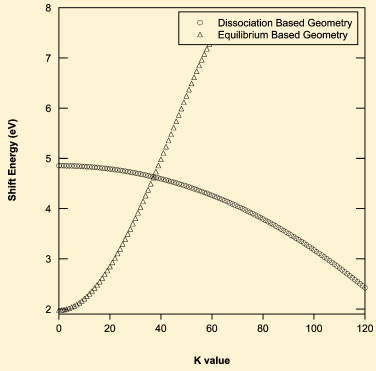

I.. INTRODUCTION

The hydroperoxyl radical, HO_2, has received very substantial experimental[1−7] and theoretical[8−51] interest over the last two decades. Far from abating over time, this interest seems only to have increased in recent years. Despite the large body of previous work, HO_2 is still regarded as dynamically "elusive",[43,44] presenting as yet unresolved challenges for rigorous quantum theoretical treatment. Serving as a reaction intermediate, this radical is an extremely key player in combustion chemistry, with the specific reaction

$$OH(^2\Pi) + O(^3P) \rightarrow H(^2S) + O_2(^3\Sigma_g^-) \quad (1)$$

being widely recognized as singularly important.[42,52] Accordingly, rate constants and/or cross sections for reactions such as eq 1 have been extensively assessed, using a variety of means. In this context, the resonance states of HO_2 are obviously very relevant. However, the bound states may also play an important (albeit indirect) role in chemical reactivity, via Lindemann-type (dissociation)/recombination mechanisms, relying on energy transfer through nonreactive third-body collisions. At any rate, the bound vibrational states of HO_2 have been extensively investigated previously, using accurate quantum dynamical techniques.[11,12,14,16,20−27,29,33,34,41]

On the other hand, it is the *rovibrational* states that are relevant for reactivity—that is, not just the vibrational states corresponding to total angular momentum $J = 0$. Accurate quantum dynamical characterization of rovibrational states is in general much more difficult. In practice, approximations are often used to characterize the rovibrational energy levels, in terms of the rotational quantum numbers J and K, and generally based on the assumption of separability of rotation and vibrational motions (and thus additivity of the corresponding energies). In particular, J. M. Bowman is the progenitor of the famous and very useful "J-shifting" [and related adiabatic rotation (AR)] approach,[13,18,19,37,40,45,46,53−57] whereby $J = 0$ results are computed exactly and used to approximate corresponding $J > 0$ results via an energy shift associated with the (usually symmetric) rigid rotor kinetic energy. This idea can be applied to the computation of reactive scattering cross sections, as well as rovibrational spectra.

In its simplest incarnation, the rigid rotor constants correspond to a single equilibrium geometry and are thus taken to be the same for all quantum states. More sophisticated versions of J-shifting allow for *state-dependent* rotational constants. In particular, Bowman's AR method leads to a vibrational-state-dependent (VSD) J-shifting scheme, for which the rotational constant values for a given rovibrational state depend on the corresponding vibrational state[13,37,55]—assuming that the latter can be meaningfully assigned. Likewise, in 1998, author B. Poirier developed a different, rotational-state-dependent (RSD) J-shifting scheme, for which the rotational constants themselves depend on J and K—thus naturally incorporating centrifugal distortion and other

Special Issue: Joel M. Bowman Festschrift

Received: January 31, 2013
Revised: May 22, 2013
Published: May 23, 2013

   dx.doi.org/10.1021/jp401154m | *J. Phys. Chem. A* 2013, 117, 7280−7297

effects.[56,57] RSD J-shifting was shown to provide substantially improved accuracy for the OHCl system, as compared to simple J-shifting—even when J and K values are large. Of course, all J-shifting schemes require that a given rovibrational state can be associated with a unique K value, but in the RSD case (unlike VSD), no additional assignments are required.

As all J-shifting strategies are approximations, it is important to establish under what conditions they are legitimate and/or accurate. In general, they may be expected to break down in the limit of high rotational and/or vibrational excitation, as well as for molecular systems that are inherently floppy. To what extent J-shifting is accurate for HO_2 has been the focus of some investigation over the years.[10,13,18,19,24,37,40,42−46] A related issue, also considered in this same literature, is the importance of Coriolis (K) coupling—that is, how "good" a quantum number K is. Ignoring Coriolis coupling leads to the "helicity conserving" (HC) approximation,[31,58,59] which in general can be regarded as less extreme than J-shifting—though to some extent this depends on the choice of embedding (rotational gauge) used to define K.[13,55] Even less extreme—but still an approximation—is the practice of "K truncation",[43] whereby some Coriolis coupling is included in the quantum dynamics calculation, but only out to $|K| \leq K_{max} < J$ (whereas an exact rovibrational calculation for a given J requires all values $|K| \leq J$).

Of course, a completely rigorous characterization of the validity of the above approximations requires comparison with accurate rovibrational quantum dynamics calculations, as well as a determination of the relevant J range. Although such calculations have been performed for the HO_2 $J = 0$ states using a variety of different potential energy surfaces (PES's),[8,9,11,12,14,16,20−27,29,33,34,39−42,46] comparatively few exact rovibrational bound state calculations have thus far been performed.[29,34−38,49,50] This is despite much evidence[13,31,32,35−37,40,42−46] suggesting that HO_2 exhibits substantial Coriolis coupling and otherwise floppy behavior. An important contributing factor here is the extremely large J values that are in practice relevant for this system. In the present paper, we show that bound rovibrational states exist at least as far as $J = 120$ (but disappear by $J = 130$). Reactive scattering applications may be expected to require even larger J values, in order to achieve fully converged results.

When Coriolis coupling is significant, K truncation may in principle still be used to reduce the computational cost. However, previous work suggests that even mild K truncation may not be so effective for HO_2 at the larger J values[31,32,43,44,46]—leading, for example, to an alternate O−OH embedding strategy[43] (as opposed to the usual embedding that adopts the O−O vector as the body-fixed z axis). Even for very low J values ($J \leq 3$), the need to include all K values in previous HO_2 bound rovibrational state calculations necessitated use of a parallel (albeit not *massively* parallel) computing strategy.[29,34−37] Consequently, the largest J value that has thus far been considered in this context prior to the present work is only $J = 50$[37]—which, though "heroic," is far from the maximum J value required. In the scattering context, the importance of large-J contributions has been recognized for some time, with gradual but steady progress having been achieved over the years, also with the help of (nonmassive) parallel computing.[31−33,39−48] In 2008, Guo and co-workers performed a $J = 150$ calculation,[43] but with the rather severe truncation of $K_{max} = 20$ (justified via the alternate embedding described above). These authors and others[43,46−48] have since performed fully Coriolis coupled (no K truncation) quantum dynamics calculations up to $J = 84$, which is particularly impressive inasmuch as state-to-state cross sections are computed, as opposed to more integrated/summed scattering quantities. In any event, this previous work clearly addresses the need to include all K values in the calculation.

The accuracy achieved in the scattering context is far less than that required in a spectroscopic calculation of rovibrational levels. In this paper, we present energy levels and wave functions for the rovibrational bound states of HO_2, computed across the entire range of J values for which these states exist, and a little beyond. These calculations have been performed using "exact" quantum dynamics—that is, no approximations beyond Born−Oppenheimer have been applied—including no K truncation, so that all Coriolis coupling is included explicitly. The results have also been converged to a much higher level of accuracy than observed in previous calculations—that is, to 10^{-6} eV or better. In particular, calculations have been performed for every multiple-of-ten J value from $J = 10$ to $J = 130$—thus filling an existing gap in the knowledge base, in that no exact $J > 50$ bound state spectroscopic calculations have ever previously been performed, to the authors' knowledge.

Together with the use of the double many-body expansion (DMBE) IV PES,[9] the focus on multiple-of-ten J values enables direct comparison with previous bound rovibrational calculations performed by Smith and co-workers up to $J = 50$, as well as with a recent article from our own group addressing the $J = 0−10$ states[50] (hereinafter referred to as "Paper I[50]"). Note that more recent and accurate PES's exist, as described in Section III, but have not been used as extensively as DMBE IV in the context of bound rovibrational states. Of particular interest in the most recent HO_2 literature have been studies addressing the density of states (DOS).[38,49] The latter work shows marked DOS differences across the different PES's, particularly at high energies. DMBE IV is found to have the highest DOS of the PES's considered—implying that the exact calculations as presented here would be substantially less computationally expensive, if performed using a more recent PES.

Despite their inherent computational difficulty, the accurate bound rovibrational state calculations of this paper have benefited very substantially from use of the ***ScalIT*** suite of codes.[50,60−64] These are a set of numerical algorithms designed to enable accurate quantum dynamics calculations to be performed effectively on massively parallel supercomputers. At the heart of ***ScalIT*** lie the routines that parallelize large sparse matrix operations (for iterative linear solvers and eigensolvers)—although various other highly efficient techniques are also employed, such as the phase space optimized discrete variable representation (PSO DVR),[65−68] preconditioned inexact spectral transform (PIST),[69−71] optimal separable basis (OSB) preconditioning,[56,72−74] and Wyatt (W) preconditioning.[71,75]

We are not the first to have applied parallel quantum dynamics techniques to the rovibrational HO_2 system—in fact, the history of the former has "paralleled" calculations of the latter since the earliest days that such techniques were developed.[29−32,76] The main strategy used—in effect, to assign one K block to each core or node—is by and large that still adopted in more recent studies, such as those from the Smith and Guo groups.[33−46] ***ScalIT***, on the other hand, adopts an entirely different approach—a much more powerful, flexible, and scalable strategy, focused on parallelization at the matrix-vector product level, and thus allowing for true, distributed-memory, massive parallelization. (See Paper I[50] for additional

discussion, both of the history of parallel quantum dynamics calculations, as well as *ScalIT* itself.) Note that HO_2 rovibrational state calculations even as low as $J = 10$ are *extremely* challenging; Smith once estimated that roughly *one-half year* would be required on a single 1.9 GHz Pentium 4 CPU. Here, using *ScalIT*, we are able to perform even one of the largest ($J = 120$) calculations on a single Intel Xeon node (two 2.66 GHz hex-core CPUs) in less than six hours. HO_2 may thus be regarded as a "small" application for *ScalIT*—although in order to test parallel scalability, we have also performed some calculations across an artificially large number of cores (up to 1200 or so). In any event, *ScalIT* is currently also being applied to much more challenging tetraatomic and pentaatomic molecular applications.

The HO_2 bound rovibrational energy levels as computed in this paper have also been used to rigorously evaluate the efficacy of VSD and RSD J-shifting across the now fully extended J range. Part and parcel with this analysis is the extent to which reasonable K labels can be legitimately assigned, which is also considered. Previous work by Smith and co-workers[37] found the performance of VSD J-shifting to be rather modest, even for the single vibrational excitation bands. Moreover, higher vibrational excitation was found to rapidly lead to deterioration of this approach, due to floppiness associated with the low-lying DMBE IV barrier to linear geometry[38] (although later authors claim that the tee-shaped transition state[51] is lower energy; the equilibrium ground state of HO_2 is in any case bent). As expected, performance was also found to diminish with increasing J, up to the highest, $J = 50$ value considered by those authors. By that point, however, even the HC approximation (i.e., the validity of the quantum label K) was found to be breaking down. More importantly, these authors conclude that the J-shifting and HC approximations are incapable of providing an indication of their own limitations and thereby avoiding the need for expensive exact quantum calculations.

Our own work as presented here and elsewhere corroborates and enhances the findings of Smith (and less directly, Guo) and co-workers. Although a comprehensive comparison of different J-shifting schemes as applied to the HO_2 bound rovibrational energy levels will form the subject of a future publication, we do provide in this paper a comparison of VSD vs RSD J-shifting for $J = 50$. Based on the above discussion, this is perhaps beyond the point where any J-shifting scheme might be expected to operate effectively. Nevertheless, our RSD scheme is found to be at least 1 order of magnitude more accurate than VSD, with many predictions within a few meV of the correct values. We also present a detailed characterization of a $J = 120$ rovibrational wave function, in terms of an underlying RSD J-shifting description. Even in this extreme context, the latter picture is found to provide valuable dynamical insight—although not necessarily a very accurate prediction of the energy levels, per se. Indeed, as discussed in Section IV, this analysis also sheds some dynamical light on the scattering case as well.

The remainder of this paper is organized as follows. Section II briefly describes the theoretical framework for the rovibrational calculations of triatomic molecules in Jacobi coordinates (Section II A) and discusses the use of the *ScalIT* codes to compute rovibrational states for triatomic molecules (Section II B). It also explains the basic operation of the VSD and RSD J-shifting strategies used here (Section II C). Section III presents numerical details for the specific *ScalIT* HO_2 bound rovibrational state calculations of this paper. Results and discussion are then presented in Section IV, including tables of rovibrational energy levels (Section IV A), analysis of J-shifting for $J = 50$ (Section IV B), and analysis of a $J = 120$ wave function (Section IV C). Finally, a summary and concluding remarks are provided in Section V.

II. THEORY AND BACKGROUND

A. Rovibrational Calculations for Triatomic AB_2 Molecules. Below we present the standard framework for rovibrational calculations of triatomic AB_2 molecules for which Jacobi coordinates, (r, R, θ), and symmetry adaptation are employed. As this is a well-established theory,[77] only the briefest of reviews is provided here. Referring all vector quantities to the body-fixed frame, the Hamiltonian is given as

$$\hat{H} = -\frac{1}{2\mu_R}\frac{\partial^2}{\partial^2 R} + \frac{1}{2\mu_R R^2}(\vec{J} - \vec{j})^2 - \frac{1}{2\mu_r}\frac{\partial^2}{\partial^2 r} + \frac{1}{2\mu_r r^2}\vec{j}^2 + V(R, r, \theta) \tag{2}$$

with (for HO_2) r the distance between the two O atoms, R the distance between H and the O−O center of mass, and θ the angle between the vectors $\vec{R}$ and $\vec{r}$. The vector $\vec{J}$ is the triatomic angular momentum, whereas $\vec{j}$ is the angular momentum associated with the diatom vector $\vec{r}$. There are also the reduced masses, μ_R and μ_r, defined as

$$\mu_r = \frac{m_O m_O}{m_O + m_O} = \frac{m_O}{2}$$
$$\mu_R = \frac{m_{O_2} m_H}{m_{O_2} + m_H} = \frac{2m_O m_H}{2m_O + m_H} \tag{3}$$

with m_O and m_H, respectively, the masses of the O and H atoms.

The ground state geometry for the HO_2 system is bent, and corresponds to a prolate (but slightly asymmetric) rigid rotor. Due to the large m_O/m_H mass ratio, the smallest moment of inertia aligns roughly with $\vec{r}$, which is thus taken as the body-fixed z-axis. This leads to the rotational quantum numbers J and K in the usual fashion—although the latter (as discussed previously) is not perfectly "good," due to Coriolis coupling. The rigorously good quantum numbers are: J, the total angular momentum; M, the projection onto the space-fixed Z axis; $\varepsilon = \pm 1$, the total inversion parity.

The rovibrational eigenstate wave functions can thus be labeled $\Psi^{JM\varepsilon}$ and expanded as[77]

$$\Psi^{JM\varepsilon}(R, r, \theta; \alpha, \beta, \gamma) = \sum_{v_1, v_2, j, K} C^{JM\varepsilon}_{v_1, v_2, j, K} \times \phi_{v_1}(R) \times \psi_{v_2}(r) \times Y^{JM\varepsilon}_{jK}(\alpha, \beta, \gamma, \theta) \tag{4}$$

with $K \geq 0$ a parity-adapted version of the usual quantum number described above, and

$$Y^{JM\varepsilon}_{jK}(\alpha, \beta, \gamma, \theta) = \sqrt{\frac{2J+1}{8\pi(1+\delta_{0K})}} \times [D^J_{MK}(\alpha, \beta, \gamma)\Theta_{j,K}(\theta) + \varepsilon D^{J*}_{M,-K}(\alpha, \beta, \gamma)\Theta_{j,-K}(\theta)] \tag{5}$$

In eq 5, D^J_{KM} are Wigner rotation matrices, $\Theta_{jK}(\theta)$ are normalized associated Legendre polynomials, and (α, β, γ) are

dx.doi.org/10.1021/jp401154m | J. Phys. Chem. A 2013, 117, 7280−7297

rotational Euler angles. In eq 4, the functions $\phi_{v_1}(R)$ and $\psi_{v_2}(r)$ are radial PSO DVRs.[65−68]

For AB_2 molecules such as HO_2, permutation of the two identical atoms is another symmetry operation to be considered. The effect on the parity-adapted combined bend-rotation angular functions is

$$Y_{jK}^{JM\varepsilon}(\alpha, \beta, \gamma, \theta) \rightarrow \varepsilon(-1)^{J-j} Y_{jK}^{JM\varepsilon}(\alpha, \beta, \gamma, \theta) \tag{6}$$

One half of these functions are thus symmetric (even) under O atom exchange; the other half are antisymmetric (odd). Since ^{16}O is a spin-zero boson, and the HO_2 ground electronic state exhibits ($^2A''$) symmetry, only those rovibrational states with odd permutation symmetry exist.

Using the basis set above, the (J, M, ε) block of the rovibrational Hamiltonian of eq 2 becomes:

$$\begin{aligned}
\mathbf{H}^{JM\varepsilon} &= H^R_{v_1v_1'}\delta_{v_2v_2'}\delta_{jj'}\delta_{KK'} + H^r_{v_2v_2'}\delta_{v_1v_1'}\delta_{jj'}\delta_{KK'} \\
&+ \left[\frac{J(J+1)-2K^2}{2\mu_R R_{v_1}^2} + \left(\frac{1}{2\mu_R R_{v_1}^2} + \frac{1}{2\mu_r r_{v_2}^2}\right) j(j+1)\right] \\
&\times \delta_{v_1v_1'}\delta_{v_2v_2'}\delta_{jj'}\delta_{KK'} \\
&- \left[\frac{\lambda_{JK}^{+}\lambda_{jK}^{+}}{2\mu_R R_{v_1}^2}\sqrt{1+\delta_{K0}}\,\delta_{K+1,K'} + \frac{\lambda_{JK}^{-}\lambda_{jK}^{-}}{2\mu_R R_{v_1}^2}\sqrt{1+\delta_{K1}}\right. \\
&\left.\delta_{K-1,K'}\right] \times \delta_{v_1v_1'}\delta_{v_2v_2'}\delta_{jj'} \\
&+ [V^K_{jj'}(R_{v_1}, r_{v_2}) - V_R(R_{v_1})\delta_{jj'} - V_r(r_{v_2})\delta_{jj'}] \\
&\times \delta_{v_1v_1'}\delta_{v_2v_2'}\delta_{KK'}
\end{aligned} \tag{7}$$

where

$$\begin{aligned}
\lambda_{JK}^{\pm} &= \sqrt{J(J+1) - K(K\pm 1)} \\
\lambda_{jK}^{\pm} &= \sqrt{j(j+1) - K(K\pm 1)} \\
V^K_{jj'}(R_{v_1}, r_{v_2}) &= \left(\frac{1+\varepsilon\delta_{K0}}{1+\delta_{K0}}\right)\langle\Theta_{jK}(\theta)|V(R_{v_1}, r_{v_2}, \theta)|\Theta_{j',K}(\theta)\rangle
\end{aligned} \tag{8}$$

and $V_R(R)$ and $V_r(r)$ are the PSO "effective potentials" in R and r, respectively (used to generate the corresponding PSO DVRs[65−68]).

B. Using *ScalIT* for Triatomic Rovibrational Spectroscopy Calculations: A Practical Guide. As the "***ScalIT***" acronym—which stands for "Scalable Iteration"—implies, ***ScalIT*** is a collection of software modules designed to scale large sparse iterative matrix manipulations across supercomputers with tens or hundreds of thousands of cores. It has primarily been envisioned as a cyberinfrastructure tool for true massively parallel, distributed-memory quantum dynamics calculations.[60−63] In this context, ***ScalIT*** represents a very substantive—and notoriously difficult—advance beyond existing small-scale parallelization strategies, which either confine themselves to (essentially trivial) shared-memory parallelization within a single compute node, or apply the K-block strategy discussed in Section I.[29−32,76,78,79]

The ***ScalIT*** codes are written in Fortran 90 and in level 2 MPI. The modular design renders it relatively easy for code developers to single out individual software components, as needed for specific functionality. Thus, other expert quantum dynamics users are free to incorporate ***ScalIT's*** sparse matrix−vector product routines into their own Lanczos,[80] quasiminimum residual[81] (QMR), filter diagonalization,[23] or time-dependent wavepacket codes, thereby introducing massively parallel functionality into these other methods. Efforts along these lines are already underway.

On the other hand, an equally important goal of the ***ScalIT*** project is to bring accurate quantum dynamics calculations within the purview of the broader chemical dynamics community, who do not necessarily have computational expertise in this area but are nevertheless desirous of accurate dynamical results. For the benefit of these nonexpert users, the ***ScalIT*** codes were designed to be very easy to use when performing certain standard computations (more so, e.g., than most electronic structure codes)—even as they provide excellent numerical performance (especially vis-à-vis parallel scalability). One such standard computation is the accurate calculation of any or all bound rovibrational eigenstates (energy levels and wave functions) for arbitrary triatomic molecules. By now, ***ScalIT*** has been successfully applied in this "non-expert" fashion to a number of highly challenging triatomic systems[50,64,82,83]—including those such as SO_2 and Ar_3 for which all atoms are "heavy." In all such cases, ***ScalIT*** has been able to reliably compute the rovibrational eigenstates to high accuracy, within a reasonable time frame, on modestly sized computing clusters.

For the benefit of the prospective nonexpert ***ScalIT*** user—for example, experimentalists interested in performing their own accurate rovibrational spectroscopy calculations, or ab initio practitioners looking to quickly validate triatomic PES's as these undergo development—we present a practical, step-by-step user's guide, as Supporting Information to this paper.

C. *J*-Shifting Strategies. In Paper I[50], the low-lying ($J \leq 10$) rovibrational eigenenergies as computed using ***ScalIT*** were assigned K values and used to compute (VSD) rotational constants for HO_2.[50] The results are in surprisingly good agreement with a previous calculation[29] that used only $J = 0$ and $J = 1$ rovibrational data. In this paper, we use various J-shifting schemes to do the reverse; a rotational energy shift associated with the rigid rotor kinetic energy is added to an exact $J = 0$ vibrational state energy, in order to estimate the energy of a corresponding rovibrational state.[13,18,19,37,40,45,46,53−57] The accuracy of the J-shifting predictions are then established via direct comparison with the corresponding exact rovibrational levels obtained using ***ScalIT***, once the latter have been assigned K labels. The K assignment is clear for the low-lying J values but starts to becomes a bit ambiguous for the larger J values.

Throughout this paper, the symmetric rigid rotor form of the rotational kinetic energy shift is presumed. This can be rationalized via the slightly asymmetric-prolate-top arguments of Section II A, but also by the fact that the earlier work as described in the previous paragraph[29,50] found the two small rotational constants to be nearly identical. In any event, the symmetric rigid rotor form leads to

$$\begin{aligned}
E_{v\,\mathrm{JK}}^{J-\mathrm{shift}} &= E_v + E_{JK}^{\mathrm{rot}} \qquad \text{where} \\
E_{JK}^{\mathrm{rot}} &= (A-B)K^2 + BJ(J+1)
\end{aligned} \tag{9}$$

as the J-shifting prediction for the true rovibrational energy E_{vJK}, in terms of the vibrational energy E_v, the rotational state (J,K),

dx.doi.org/10.1021/jp401154m | J. Phys. Chem. A 2013, 117, 7280−7297

and the rotational constants, A and B. For the presumed prolate HO_2 rigid rotor, $A > B$.

Different J-shifting schemes may be distinguished with regard to how the values of A and B are determined (or more generally E_{JK}^{rot}; an upcoming paper will explore quite a number of options). The simplest choice is to use the moments of inertia associated with the HO_2 equilibrium ground state geometry, to obtain one set of rotational constants for use with all rovibrational states. Though necessarily asymmetric, the two small rotational constants (being nearly identical as discussed above) can be simply averaged together to obtain the symmetric rotor form of eq 9.[13,37,54,55]

Of course, the rotational constants can also be determined experimentally. In this context, a more refined and commonly employed spectroscopic technique is to allow the rotational constants to depend on the vibrational state, v, giving rise to a VSD J-shifting scheme. Using $A(v)$ and $B(v)$ values for the ground and lowest two singly excited vibrational states of HO_2 as obtained from earlier experimental work of Burkholder and co-workers,[84] the Smith group applied VSD J-shifting to the lowest-lying dozen or so rovibrational states (of each parity) for $J = 50$.[37]

In this paper, we explore an RSD J-shifting scheme, for which the rotational constants depend on the rotational, rather than vibrational, state. Again, a similar strategy may be found in standard spectroscopic analysis, where centrifugal distortion and related effects are incorporated via higher-order J and K terms in the rotational kinetic energy expansion. Rather than obtaining the expansion parameters via fitting to experimental data, however, we rely on a more natural and purely theoretical determination of the E_{JK}^{rot} values. This leads to a cleaner and more self-consistent assessment of the efficacy of the J-shifting approach (since the PES may itself exhibit discrepancies vs experimental data) and—for the HO_2 example at least—far better performance than for VSD J-shifting.

The RSD J-shifting scheme is based on an alternate—and in many respects more natural—form of the exact rovibrational quantum Hamiltonian that was first derived by author B. Poirier in 1998.[56,57,85] One feature of this approach is that it automatically generalizes the two-body notion of the "centrifugal potential" for three-body systems. Among other benefits, this allows for a true direct-product basis representation of the rovibrational Hamiltonian, using a single K-independent bend-angle basis set—as was once advocated by Bowman himself,[13] and successfully applied to real molecular systems by Poirier[85] (though the traditional K-dependent basis of eq 4 is used in the present work).

As might be expected via analogy with the two-body case, the three-body centrifugal potential depends on the triatomic internal coordinates, (R,r,θ), as well as the rotational state indices, (J,K). Also, it is added directly to the true potential, to obtain the "effective potential" governing the dynamics for a given rotational state. The explicit formula for the latter is found to be[56,57]

$$V_{JK}^{\mathrm{eff}}(R, r, \theta) = V(R, r, \theta) + \frac{J(J+1)}{2\mu_r r^2} + \left(\frac{1}{2\mu_R R^2 \sin^2\theta} + \frac{\cot^2\theta - 1}{2\mu_r r^2}\right)K^2 \quad (10)$$

in units where $\hbar = 1$, as are presumed throughout this paper.

Curiously, the centrifugal potential energy in eq 10 has the form of a symmetric rigid rotor for all geometries—even though the actual three-body rotor is generally asymmetric. In any event, to extract a meaningful RSD J-shifting approximation from eq 10, one simply minimizes $V_{JK}^{\mathrm{eff}}(R, r, \theta)$ rather than $V(R, r, \theta)$ itself, with respect to the internal coordinates, for each rotational state (J,K). The resultant RSD energy shift—that is, E_{JK}^{rot} in eq 9—is then taken to be $\{\min[V_{JK}^{\mathrm{eff}}(R, r, \theta)] - \min[V(R, r, \theta)]\}$, where the two minima are evaluated independently. Note that this differs slightly from the scheme proposed in ref 56, for which *both* V and V_{JK}^{eff} are evaluated at the minimum geometry of the latter.

III. COMPUTATIONAL DETAILS

A number of PES's may be found in the HO_2 literature[8,9,15,39−42] (for an overview, consult Paper I[50]). As per Section I, however, we use the DMBE IV PES in the present work. This PES was used in all previous HO_2 rovibrational state calculations,[29,34−37,50] with which we wish to compare our results. Since the system and PES are the same as in Paper I[50], the radial PSO effective potentials, $V_R(R)$ and $V_r(r)$, are also the same as were used in Paper I[50] (Sec. II A; the interested reader is referred to Figure 1 of Paper I[50]). The radial sinc-DVR grid[86] used is also the same, that is, 6000 uniformly spaced points in both R and r, across the coordinate ranges indicated in Table 1.

Table 1. Parameters Used for All HO_2 Bound Rovibrational Eigenstate Calculations Presented in This Paper[a]

category	parameter	value (au)
mass	μ_r	14578.471659
	μ_R	1781.041591
coordinate ranges	r_{min}	1.0
	r_{max}	11.0
	R_{min}	0.0
	R_{max}	11.0

[a]All units are atomic units.

In Paper I[50], the number of radial PSO DVR points used was $N_R = 60$ for coordinate R and $N_r = 40$ for coordinate r. Comprehensive convergence testing indicated that these values correspond to final computed HO_2 rovibrational energies that are all converged to better than 10^{-6} eV—including the highly vibrationally excited states close to the dissociation threshold, as well as rotationally excited states corresponding to the highest J value considered ($J = 10$). As a comparison, Smith and co-workers used a standard PO DVR of size $(N_R = 110) \times (N_r = 50)$, contracted from a 315×150 primitive sinc-DVR grid,[23] for both their low-J[35,36] and high-J[37] HO_2 rovibrational state calculations. Despite using more than twice as many radial DVR functions as we did, their calculations achieve significantly less accuracy than the present work (their stated accuracy was 10^{-5} eV or so, although comparison with our results suggests 10^{-4} eV or better, for the larger J values). This is a testament to the efficacy of the PSO DVR approach and in line with what we have observed previously using this method.

In the present paper, we compute the lowest-lying 30 bound rovibrational eigenstates, for each J and ε value considered. For $J < 90$, these states lie sufficiently far from the dissociation threshold that substantially fewer radial PSO DVR points are required than was the case in Paper I[50]. This is indicated in Columns II and III of Table 2, which list the number of radial PSO DVR points in r and R, respectively, required to converge

dx.doi.org/10.1021/jp401154m | J. Phys. Chem. A 2013, 117, 7280−7297

Table 2. Basis Sizes Used for Various HO_2 Bound Rovibrational Eigenstate Calculations Presented in This Paper, as a Function of Total Angular Momentum, J: N_r, the Number of Radial PSO DVR Points in r; N_R, the Number of Radial PSO DVR Points in R; j_{max}, the Number of Bend-Angle (θ) Basis Functions; jK_{num}, the Number of Combined Bend-Rotation Basis Functions[a]

J value	N_r	N_R	j_{max} value	jK_{num} value
10	22	24	90	600
20	22	24	90	600
30	22	24	90	650
40	22	26	90	650
50	22	26	90	650
60	24	26	90	650
70	30	50	120	800
80	30	50	120	800
90	40	60	130	1000
100	40	60	130	1000
110	40	60	130	1000
120	50	60	200	1000
130	50	60	225	1000
50 (highest-lying)	30	40	120	900

[a]These were used to achieve convergence of all computed eigenvalues to 10^{-6} eV or better.

all of the computed energy eigenvalues at the specified J value to 10^{-6} eV or better. On the other hand, the $90 \leq J \leq 110$ PSO DVR grid sizes match those of Paper I[50], and the $J = 120$ and $J = 130$ PSO DVR grid sizes slightly *exceed* the older values. This situation will be further commented upon below.

In the highest-J calculations that were performed by Smith and co-workers,[37] the lowest-lying 12−15 rovibrational states of each parity for $J = 30$, 40, and 50 were computed and assigned K and v labels. Separate low-J studies provided similar data for $J = 10$ (but without the v labels),[35] and for $J = 20$ (with neither v nor K labels). Note that these results encompass only the lowest two vibrational excitations. It should be mentioned that ref 37 also includes some high-lying eigenstates for each of the three J values—although these defy all attempts at labeling. In any event, their low-lying results may be directly compared with those of the present paper—as the same DMBE IV PES was used, and no K truncation was applied. The v label assignments enable use of VSD J-shifting, as was applied and assessed in ref 37. A similar calculation is performed in this paper for the $J = 50$, $\varepsilon = 0$ (even parity) rovibrational states—but using RSD J-shifting, and our own K assignments.

The final convergence parameter impacting the accuracy of the HO_2 energy level calculation is j_{max}—the maximum value for j in eq 7, and (essentially) the number of bend-angle basis functions. To achieve a final level of convergence comparable to that of the radial PSO DVR, the j_{max} values indicated in Table 2 were employed. As j_{max} must be larger than J itself—provided no K truncation is applied, as is the case here—one expects a marked J dependence, as is indeed observed in the table. Together with the expanded K range, this is the reason that larger J values lead to much more expensive calculations. A more direct measure of this increase, however, is to be found in jK_{num}—the total number of combined bend-rotation basis functions used in the calculation—whose values are provided in Column V of Table 2. In comparison with the high-J calculations of Smith and co-workers, our angular basis sizes are significantly larger—reflecting the fact that the underlying basis functions are (essentially) the same in both calculations, but our calculation is performed to substantially higher accuracy. Note that their calculation introduces quadrature error in the potential energy matrix elements through the use of an associated Legendre DVR grid, which may also affect the accuracy of their results.

All in all, the total basis size used by Smith and co-workers for their largest $J = 50$ calculation was around 5.7×10^6, whereas our corresponding largest $J = 50$ basis is 1.08×10^6. They used the same basis for both their low- and high-lying energy window calculations. In our case, we singled out the high-lying HO_2 bound rovibrational states of $J = 50$ for special consideration, as potentially the most computationally challenging of all. In general, increasing J increases the required number of combined bend-rotation states (Table 2), making the calculation more difficult; but at the same time, it also leads to a shallower effective potential well (eq 10), making the calculation easier. The "worst of both worlds" is therefore likely to be found in the middle of the J range—for example, around $J = 50$. In any event, we have performed $J = 50$ calculations for a number of spectral windows at successively higher energies—with the largest basis size as reported above that used for the highest-lying window. As it happens, the $J = 120$ calculation required an even larger basis size, owing to the presence of states just below the dissociation threshold—although the highest-lying $J = 50$ calculation was still the more computationally expensive, owing to the increased number of QMR iterations (Section IV A).

We note that we have conducted many hundreds of convergence tests, considering each value of J separately, to ensure the validity of all of our computed results. Smith and co-workers performed accurate convergence testing for $J = 0$, and then used the same converged radial basis sizes for all of their larger J calculations. Equation 10 suggests that this should in fact be a legitimate strategy—since the effective potential is (virtually always) positive, and the same number of states is being computed for each J. Of course, such an analysis is only valid so long as the computed eigenstates are far from the dissociation threshold—when the latter is approached, one expects larger PSO DVR grids to be required, perhaps on the order of the largest $J = 0$ grids from Paper I.[50] Our own work leads to a slightly different conclusion, however. From Table 2, we find that: (1) radial PSO DVR grid sizes must be increased throughout the J range, not just at the highest values where dissociation is approached; (2) the highest J values require slightly larger radial PSO DVR grids than in Paper I.[50] The underlying reasons are not entirely clear, but may have to do with the fact that increasing J results in an effective potential well that is *broader*, as well as shallower.

Parallel scalability of the HO_2 ***ScalIT*** calculations was also investigated. By the standards of many iterative sparse matrix calculations, the total basis size required for even one of the largest ($J = 120$) calculations performed here—that is, 2.5×10^6—is quite modest. Consequently, the bottleneck, stage 3 component of even this $J = 120$ calculation can be performed on a single Intel Xeon node (two 2.66 GHz hex-core CPUs) in less than six hours. For convenience however, most of the larger of the calculations were parallelized across five nodes, or 60 cores. The corresponding parallel speedup observed for the above $J = 120$ calculation was about 45×, corresponding to an excellent parallel efficiency of 75.4%—despite the small problem size, and the significant amount of distributed memory

Table 3. Lowest-Lying Rovibrational Energy Levels of HO_2 for Total Angular Momentum $J = 10$, with Odd Permutation Symmetry and Both Even and Odd Parity[a]

index	even parity				odd parity			
n	K	Smith/LHFD	Poirier/2010	this work	K	Smith/LHFD	Poirier/2010	this work
1	0	0.014855	0.014863	0.0148635	1	0.017474	0.017480	0.0174802
2	1	0.017049	0.017058	0.0170575	2	0.024455	0.024461	0.0244614
3	2	0.024463	0.024473	0.0244729	3	0.036425	0.036433	0.0364339
4	3	0.036426	0.036436	0.0364361	4	0.053143	0.053153	0.0531532
5	4	0.053143	0.053156	0.0531555	5	0.074573	0.074586	0.0745858
6	5	0.074573	0.074588	0.0745881	6	0.100669	0.100685	0.1006848
7	6	0.100669	0.100687	0.1006871	7	0.131375	0.131394	0.1313944
8	7	0.131375	0.131396	0.1313967	1	0.149204	0.149224	0.1492244
9	0	0.146616	0.146635	0.1466357	2	0.156098	0.156119	0.1561186
10	1	0.148782	0.148801	0.1488015	3	0.166628	0.166651	0.1666509
11	2	0.156107	0.156127	0.1561274	8	0.167922	0.167944	0.1679447
12	8	0.166628	0.166653	0.1666532	1	0.178402	0.178415	0.1784157
13	3	0.167922	0.167944	0.1679443	4	0.184436	0.184461	0.1844606
14	0	0.175663	0.175679	0.1756787	2	0.185646	0.185660	0.1856603
15	1	0.177932	0.177947	0.1779468	3	0.198090	0.198106	0.1981061
16	4	0.184436	0.184460	0.1844602	5	0.205607	0.205633	0.2056337
17	2	0.185656	0.185673	0.1856730	9	0.206335	0.206383	0.2063827
18	3	0.198090	0.198108	0.1981079	4	0.215462	0.215479	0.2154794
19	5	0.205607	0.205633	0.2056333	6	0.231388	0.231417	0.2314174
20	9	0.206355	0.206385	0.2063850	5	0.237720	0.237741	0.2377409
21	4	0.215461	0.215481	0.2154813	10	0.250479	0.250512	0.2505115
22	6	0.231388	0.231417	0.2314170	7	0.261717	0.261750	0.2617504
23	5	0.237720	0.237743	0.2377428	6	0.264817	0.264842	0.2648418
24	10	0.250479	0.250514	0.2505137	1	0.276003	0.276039	0.2760385
25	6	0.261717	0.261750	0.2617501	2	0.282813	0.282850	0.2828497
26	7	0.264818	0.264844	0.2648437	3	0.294493	0.294534	0.2945335
27	0	0.273446	0.273480	0.2734798	7	0.296302	0.296334	0.2963343
28	1	0.275586	0.275620	0.2756196	8	0.296923	0.296953	0.2969525
29	2	0.282822	0.282857	0.2828565	1	0.309843	0.309870	0.3098703
30	3	0.294496	0.294530	0.2945330	4	0.310810	0.310852	0.3108521

[a]All energies are in eV and relative to the vibrational ground state. Previous results from Paper I[50] and from Smith et al.[35] are also presented. New energies are converged to 10^{-6} eV or better; they agree with Paper I[50] to this level of accuracy, and with ref 35 to within 10^{-4} eV or better. Columns II and VI: our K assignments. These agree with Paper I,[50] except for the even parity $n = 25$ and 26 assignments, which are switched.

parallelization. As an explicit test of scalability, we further parallelized this same calculation (up to 10 nodes, or 120 cores), leading to a maximum parallel speedup of around 66×. In contrast, the best speedup achieved by Smith and co-workers was around 6×—even though they used only shared, not distributed, memory parallelization.

The calculations described above were performed on the Robinson cluster (Texas Tech University Department of Chemistry and Biochemistry). Although HO_2 presents a "small" application vis-à-vis massive parallelization, some scalability tests across a much larger number of nodes were also performed—using the Lonestar cluster (Texas Advanced Computation Center), which has a similar architecture as Robinson (12 cores per node and low-latency, high-bandwidth Infiniband connectivity). Even though the HO_2 application size was not increased, effective parallel scalability was achieved across 100 or so Lonestar *nodes*. However, this study also revealed some inefficiency in the combining of shared and distributed parallelization in the second phase of stage 3 (Section II B) that bears further investigation.

IV. RESULTS AND DISCUSSION

A. Rovibrational Eigenstates. Using *ScalIT*, bound rovibrational energy levels of HO_2 were computed for all multiple-of-ten J values, up to the largest J for which bound states exist ($J = 120$) and a bit beyond ($J = 130$). Only states with odd permutation symmetry were considered, as nuclear spin-statistics rule out the physical existence of the even permutation symmetry states. However, both even and odd parity states were computed for each J value considered. For each J and parity value, the lowest-lying 30 rovibrational energies were obtained from a single PIST spectral window calculation.[69−71] For $J = 50$ with even parity, a number of higher-lying spectral window calculations were also performed, in order to compute the lowest-lying 125 states. All rovibrational energies are reported in eV, relative to the vibrational ground state energy from Paper I.[50]

Each calculation typically required around 100 Lanczos iterations, and 15 QMR iterations per Lanczos iteration—or 1500 iterations total—to converge the 30 states. This is with a typical Wyatt window size of around 50 states (a larger window would have led to fewer QMR iterations, but greater computational cost for the preconditioner construction). In contrast, Smith and co-workers required from 10^5 to 10^6 iterations to converge each of their filter diagonalization calculations[37,38]—although their computational cost per iteration is somewhat less than ours. For so many iterations—arguably the largest ever published at the time—

dx.doi.org/10.1021/jp401154m | J. Phys. Chem. A 2013, 117, 7280−7297

reorthogonalization of the Lanczos vectors is certainly not possible,[80] and so those authors must contend with spurious eigenvalues and other headaches.

Regardless of the iterative method used, the number of iterations increases with increasing spectral energy. For our even-parity J = 50 calculations, for instance, around 400 QMR iterations per Lanczos iteration were required for the highest-lying spectral window considered, using a Wyatt window of 750 states. Consequently, these were the most time-consuming of our calculations (13.9 h across 36 cores), even though the basis size was smaller than for J = 120 and J = 130, as indicated in Table 2.

For J = 120, the attractive PES well is nearly obliterated by the centrifugal potential, and so the effective potential of eq 10 is very shallow. Only around 20 bound rovibrational eigenstates of each parity were obtained for this J value. For J = 130, a large-basis calculation found no rovibrational eigenstates for either parity; the converged even-parity ground state, for example, was found to lie at 7.69×10^{-2} eV above the H + O_2 dissociation threshold of 2.0158147 eV (relative to the vibrational ground state[50]). This would appear to rule out any J = 130 bound states—although it is conceivable that a new calculation with an expanded radial coordinate range might reveal the above state to be extremely weakly bound. In any event, the J = 130 calculation was performed here to confirm that we have indeed reached the end of the J range for the bound states. In the J = 120 case, in addition to computing rovibrational energy eigenvalues, ***ScalIT*** was also used to compute a representative wave function (see Section IV C for further discussion).

The HO_2 bound rovibrational energy levels for J = 10, for both even and odd parities, are presented in Table 3. These states have been previously investigated by Smith and co-workers[35] and by the present authors (Paper I[50]). The previous results are also presented here and serve as a useful check on the present results. All of the new eigenvalues agree with those of Paper I[50] to within the accuracy that those two sets of calculations were converged—that is, 10^{-6} eV or better. The agreement with Smith and co-workers is to within 10^{-4} eV or better. The K values listed in the table are our assignments, as obtained using the procedure described in Section IV B. These agree with the assignments used in Paper I[50], apart from a switching of the n = 25 and n = 26 even-parity labels, where n labels the rovibrational state excitation.

The HO_2 bound rovibrational energy levels for J = 20, for both even and odd parities, are presented in Table 4. These states have also been previously investigated by Smith and co-workers,[36] using similar methodology and basis sets as for their J = 10 study. Perhaps not surprisingly, therefore, the agreement of their results with ours is again to within 10^{-4} eV or better.

The HO_2 bound rovibrational energy levels for J = 30 and 40, for both even and odd parities, are presented, respectively, in Tables 5 and 6. Together with J = 50, these states have also been previously investigated by Smith and co-workers, in their high-J study of 2006.[37] Note that they have only computed the lowest 12−15 states of each J and parity, whereas we continue to obtain states up to n = 30. For those states for which Smith and co-workers have provided data, the computed energy levels agree to within 10^{-4} eV or better with our results, and the K assignments agree perfectly with ours.

As discussed previously, the J = 50 case is singled out for special consideration. The HO_2 bound rovibrational energy levels for J = 50 and even parity are presented in Table 7. Like the other calculations, these are converged to 10^{-6} eV or better. In this table, we provide both K and v labels—where v refers to the vibrational excitation—according to the procedure described in Section IV B. The latter label is required for VSD J-shifting, as performed in ref 37 and in this paper (along with RSD J-shifting) in Section IV B. In any event, our K and v labels agree perfectly with those of ref 37, for the 15 states for which they have provided data. The computed rovibrational energies for these states also again agree to within 10^{-4} eV or better. Similar comments also apply for the odd-parity J = 50 levels, as presented in Table 8. In Table 9, reaching about halfway up the bound spectrum, the lowest-lying 125 bound rovibrational energy levels for J = 50 and even parity are presented, obtained using multiple spectral energy windows. As discussed in Section III and above, these constitute some of the most difficult possible spectral calculations for HO_2.

Continuing along these lines, the HO_2 bound rovibrational energy levels for J = 60, 70, and 80, for both even and odd parities, are presented, in Table 10. No previous calculations exist for comparison. Also, for such large J values, we do not bother to make K value assignments. Similar results for J = 90,

Table 4. Lowest-Lying Rovibrational Energy Levels of HO_2 for Total Angular Momentum J = 20, with Odd Permutation Symmetry and Both Even and Odd Parity[a]

index	even parity			odd parity		
n	K	Smith/LSFD	this work	K	Smith/LSFD	this work
1	0	0.056551	0.0565703	1	0.059852	0.0598696
2	1	0.058240	0.0582594	2	0.066237	0.0662548
3	2	0.066369	0.0663898	3	0.078223	0.0782420
4	3	0.078220	0.0782416	4	0.094902	0.0949208
5	4	0.094900	0.0949232	5	0.116287	0.1163096
6	5	0.116287	0.1163119	6	0.142334	0.1423575
7	6	0.142333	0.1423598	7	0.172981	0.1730081
8	7	0.172981	0.1730104	1	0.190651	0.1906837
9	0	0.187386	0.1874178	2	0.196693	0.1969833
10	1	0.189058	0.1890818	3	0.208167	0.2081975
11	2	0.197082	0.1971150	8	0.208784	0.2088182
12	8	0.208167	0.2081998	1	0.221083	0.2211057
13	3	0.208930	0.2088153	4	0.225250	0.2252848
14	0	0.217634	0.2176066	2	0.227667	0.2276917
15	1	0.219282	0.2193221	3	0.240132	0.2401573
16	4	0.225250	0.2252846	5	0.246363	0.2464000
17	2	0.227822	0.2278492	9	0.247821	0.2478543
18	3	0.240130	0.2401558	4	0.257468	0.2574890
19	5	0.246363	0.2463998	6	0.272070	0.2721084
20	9	0.247821	0.2478566	5	0.279748	0.2797138
21	4	0.257462	0.2574909	10	0.291863	0.2919002
22	6	0.272069	0.2721083	7	0.302291	0.3023322
23	5	0.279680	0.2797157	6	0.306807	0.3067943
24	10	0.291863	0.2919024	1	0.316543	0.3165921
25	6	0.302293	0.3023321	2	0.322767	0.3228162
26	7	0.306762	0.3067961	3	0.334457	0.3345072
27	0	0.313319	0.3133660	7	0.336807	0.3368487
28	1	0.314994	0.3150107	8	0.338825	0.3388240
29	2	0.322896	0.3229438	1	0.340210	0.3402506
30	3	0.334454	0.3345025	4	0.350723	0.3507751

[a]All energies are in eV and relative to the vibrational ground state. Previous results from Smith et al.[36] are also presented. New energies are converged to 10^{-6} eV or better; they agree with ref 36 to within 10^{-4} eV or better. Columns II and V: our K assignments.

dx.doi.org/10.1021/jp401154m | J. Phys. Chem. A 2013, 117, 7280−7297

Table 5. Lowest-Lying Rovibrational Energy Levels of HO_2 for Total Angular Momentum $J = 30$, with Odd Permutation Symmetry and Both Even and Odd Parity[a]

index	even parity			odd parity		
n	K	Smith/ LSFD	this work	K	Smith/ LSFD	this work
1	0	0.124642	0.1246776	1	0.129246	0.1292814
2	1	0.125728	0.1257642	2	0.134702	0.1347378
3	2	0.135318	0.1353560	3	0.146814	0.1468507
4	3	0.146785	0.1468240	4	0.163395	0.1634332
5	4	0.163396	0.1634361	5	0.184703	0.1847425
6	5	0.184702	0.1847448	6	0.210660	0.2107025
7	6	0.210661	0.2107047	7	0.241209	0.2412539
8	7	0.241209	0.2412561	1	0.258503	0.2585524
9	0	0.253944	0.2539930	2	0.263879	0.2639284
10	1	0.255012	0.2550603	3	0.275937	0.2758806
11	2	0.26449	0.2645401	8	0.276284	0.2763316
12	8	0.275801	0.2758517	1	0.290950	0.2909922
13	3	0.276284	0.2763338	4		0.2922441
14	0	0.285991	0.2860331	2		0.2965573
15	1	0.287061	0.2871032	3		0.3091714
16	4		0.2922421	5		0.3132623
17	2		0.2972783	9		0.3158640
18	3		0.3091373	4		0.3263911
19	5		0.3132624	6		0.3388622
20	9		0.3158662	5		0.3485280
21	4		0.3263936	10		0.3597727
22	6		0.3388623	7		0.3689623
23	5		0.3485297	6		0.3755121
24	10		0.3597749	1		0.3829698
25	6		0.3689624	2		0.3882828
26	7		0.3755139	3		0.4000865
27	0		0.3784699	7		0.4034215
28	1		0.3795255	8		0.4073516
29	2		0.3888819	1		0.4079737
30	3		0.4000564	4		0.4162462

[a]All energies are in eV and relative to the vibrational ground state. Previous results from Smith et al.[37] are also presented. New energies are converged to 10^{-6} eV or better; they agree with ref 37 to within 10^{-4} eV or better. Columns II and V: our K assignments (agree with ref 37).

Table 6. Lowest-Lying Rovibrational Energy Levels of HO_2 for Total Angular Momentum $J = 40$, with Odd Permutation Symmetry and Both Even and Odd Parity[a]

index	even parity			odd parity		
n	K	Smith/ LSFD	this work	K	Smith/ LSFD	this work
1	0	0.218531	0.2185910	1	0.225158	0.2252188
2	1	0.219106	0.2191853	2	0.229505	0.2295107
3	2	0.231164	0.2312276	3	0.241961	0.2420222
4	3	0.241808	0.2418725	4	0.258325	0.2583874
5	4	0.25833	0.2583948	5	0.279508	0.2795725
6	5	0.279508	0.2795746	6	0.305336	0.3054022
7	6	0.305336	0.3054043	7	0.335742	0.3358109
8	7	0.335742	0.3358130	1	0.352246	0.3523197
9	0	0.345684	0.3457563	2	0.356469	0.3565420
10	1	0.346284	0.3463382	3	0.368807	0.3688821
11	2	0.358167	0.3582421	8	0.370658	0.3707302
12	8	0.368656	0.3687311	1	0.384935	0.3850113
13	3	0.370658	0.3707323	4		0.3875629
14	0	0.380266	0.3803327	2		0.3918437
15	1	0.380826	0.3808922	3		0.4049241
16	4		0.3850259	5		0.4059063
17	2		0.3938301	9		0.4100872
18	3		0.4047384	4		0.4218789
19	5		0.4059066	6		0.4313630
20	9		0.4100893	5		0.4438614
21	4		0.4218875	10		0.4538032
22	6		0.4313633	7		0.4613151
23	5		0.4438631	6		0.4706743
24	10		0.4538053	1		0.4746615
25	6		0.4613156	2		0.4788368
26	7		0.4681882	3		0.4910178
27	0		0.4687643	7		0.4956605
28	1		0.4706761	8		0.5017937
29	2		0.4805050	1		0.5022761
30	3		0.4908685	4		0.5069517

[a]All energies are in eV and relative to the vibrational ground state. Previous results from Smith et al.[37] are also presented. New energies are converged to a 10^{-6} eV or better; they agree with ref 37 to within 10^{-4} eV or better. Columns II and V: our K assignments (agree with ref 37).

100, 110, and 120 are presented in Table 11. These rovibrational energies become increasingly close to the dissociation threshold of 2.0158147 eV, with the $J = 120$ states reaching dissociation by $n \approx 20$ for both parities. As discussed, the proximity to dissociation leads to a substantially more difficult calculation. Nevertheless, we were able to converge all computed energies to our target accuracy of 10^{-6} eV or better. That said, it may be that the highest-lying rovibrational energies for $J = 120$, that is, those lying just below the dissociation threshold, might change a bit under a new calculation performed using an expanded radial coordinate range.

B. *J*-Shifting Results for $J = 50$. As discussed in Section I, the validity of the HC and *J*-shifting approximations as applied to HO_2 is a topic of perennial interest.[10,13,18,19,24,37,40,42−46] The general feeling appears to be that these are not very reliable, particularly for large J or large vibrational excitation. In this regime, the flexibility of HO_2—particularly the low transition state barriers to isomerization[37,38,51]—contributes to substantial HC breakdown. Some might argue that since the DMBE IV PES is not accurate at high energies, evaluating HC breakdown there is not relevant; however, for purely *theoretical* investigations—for example, the comparison vs exact quantum results that will be conducted here—this PES should serve perfectly well.

With regard to bound rovibrational state calculations, Smith and co-workers conclude that by $J = 50$, the validity of the label K is becoming suspect, and even vibrational assignment is only possible for the very lowest-lying excitations.[37] As a result, *J*-shifting—even VSD *J*-shifting—is unreliable, particularly for states that lie close to one another, for which *K*-mixing is especially pronounced. Another important observation, made by Bowman some years ago,[13] is that "as J and K increase, the states that were bound states become resonances"—a particularly nettlesome phenomenon, vis-à-vis *J*-shifting, that will be taken up again in Section IV C.

Recent HO_2 work pertaining to application of *J*-shifting in the reactive scattering context also bears comment. The most recent and accurate calculations by Guo and co-workers[40,43−46] again suggest that *J*-shifting is ineffective. Though less accuracy is required in the reactive scattering context, the inherent high

Table 7. Lowest-Lying Rovibrational Energy Levels of HO_2 for Total Angular Momentum $J = 50$, with Odd Permutation Symmetry and Even Parity[a]

state labels			Smith/LSFD			this work		
n	v	K	energy	VSD J-shift	error	energy	RSD J-shift	error
1	0	0	0.337633	0.343722	−0.006089	0.3377239	0.3377239	0
2	0	1	0.337923	0.346111	−0.008188	0.3380129	0.3401239	−0.002110
3	0	2	0.353452	0.353278	0.000174	0.3535472	0.3473199	0.006227
4	0	3	0.362818	0.365223	−0.002405	0.3629127	0.3592969	0.003616
5	0	4	0.379279	0.381947	−0.002668	0.3793755	0.3760269	0.003349
6	0	5	0.400257	0.403449	−0.003192	0.4003546	0.3974759	0.002879
7	0	6	0.425905	0.429729	−0.003824	0.4260047	0.4235979	0.002407
8	0	7	0.456121	0.460787	−0.004666	0.4562228	0.4543399	0.001883
9	**1**	0	0.462009	0.550546	**−0.088537**	0.4621111	0.4698269	**−0.007716**
10	**1**	1	0.462292	0.552900	**−0.090608**	0.4623934	0.4722269	**−0.009834**
11	**1**	2	0.477640	0.559962	**−0.082322**	0.4777465	0.4794239	**−0.001678**
12	0	8	0.486861	0.496624	−0.009763	0.4869664	0.4896409	−0.002675
13	**1**	3	0.490829	0.571732	**−0.080903**	0.4909338	0.4913999	**−0.000466**
14	**2**	0	0.499818	0.592906	**−0.093088**	0.4999147	0.4984539	**0.001461**
15	**2**	1	0.500070	0.595335	**−0.095264**	0.5001664	0.5008549	**−0.000689**
16	**1**	4		0.588209	**−0.085007**	0.5032023	0.5081299	**−0.004928**
17	**2**	2		0.602622	**−0.085605**	0.5170171	0.5080509	**0.008966**
18	**2**	3		0.614767	**−0.090893**	0.5238741	0.5200269	**0.003847**
19	**1**	5		0.609394	**−0.082916**	0.5264781	0.5295789	**−0.003101**
20	0	9		0.537238	−0.007176	0.5300623	0.5294299	0.000632
21	**2**	4		0.631769	**−0.088218**	0.5435514	0.5367579	**0.006793**
22	**1**	6		0.635287	**−0.086140**	0.5491468	0.5557009	**−0.006554**
23	**2**	5		0.653630	**−0.088361**	0.5652690	0.5582069	**0.007062**
24	0	10		0.582631	−0.009104	0.5735271	0.5736319	−0.000105
25	**2**	6		0.680348	**−0.101435**	0.5789125	0.5843289	**−0.005416**
26	**1**	7		0.665888	**−0.083962**	0.5819257	0.5864439	**−0.004518**
27	3	0				0.5822055	0.5969889	−0.014783
28	3	1				0.5918391	0.5993899	−0.007551
29	3	2				0.5973373	0.6065859	−0.009249
30	3	3				0.6064520	0.6185619	−0.012110

[a]All energies are in eV and relative to the vibrational ground state. Previous results from Smith et al.[37] are also presented—as are approximate VSD (Column V) and RSD (Column VIII) J-shifting results, together with corresponding errors (Columns VI and IX, respectively). Column III: our K assignments (agree with ref 37). Column II: vibrational state assignments (agree with ref 37). Boldfaced entries indicate vibrationally excited rovibrational states.

energies and molecular rearrangements pose their own problems. In addition, since the reaction involves a stable intermediate, there is also the fundamental problem—raised years earlier by Bowman[13]—of which geometry should be used for J-shifting: the transition state, or the HO_2 intermediate minimum? There is one research group[18,19] that claims that the O−OH transition state leads to a viable J-shifting strategy—one which, moreover, is alleged to work *better* at higher excitation energies. By their own admission, however, these conclusions are "controversial"; in any event, they performed no $J > 0$ calculations (and used a different PES), drawing their conclusions directly from comparison with experiment.

In contrast, Guo and co-workers argue that J-shifting must *inherently* fail for HO_2 reactive scattering applications, because the form of the energy dependence of the scattering quantities is very different from one J value to the next.[45,46] (As a side note, they also find, interestingly, that quasiclassical trajectories yield poor predictions for overall cross sections but good predictions of relative product state distributions). As a basic, inherent requirement for the success of J-shifting, the energy-dependent curves for different J values must closely resemble each other, apart from an energetic shift (although in practice, whether the shift energies may be accurately estimated *a priori* is another matter). As this is not the case for HO_2, that would seem to definitively rule out using any J-shifting scheme reliably in this context.

On the other hand, Figure 1 suggests that there is indeed hope for the HO_2 bound rovibrational states—and moreover, one that may achieve some success throughout the *entire* $10 \leq J \leq 120$ range! In the figure, each curve represents the lowest-lying 30 exact rovibrational energies (of even parity) for a given J value, presented in energetic order—as in Section IV A, but without regard to any other considerations such as state labeling. As is very evident from the figure, *these curves do indeed resemble one another*, apart from an energetic shift. Moreover, the shift energy appears to be roughly quadratic in J—that is, exactly what one would expect, based on eq 9. It is perhaps surprising that this basic pattern persists across the entire J range—even where HC breakdown is undoubtedly very severe and for rotational energies that are nearly sufficient to dissociate the molecule. That said, we note that the states in Figure 1 are all low-lying with respect to their vibrational excitation; one cannot expect the pattern to extend to the highly vibrationally excited rovibrational states. Also, although the resemblance is especially close for $J \leq 50$, the curves increasingly deviate from one another as J increases beyond this value.

dx.doi.org/10.1021/jp401154m | J. Phys. Chem. A 2013, 117, 7280−7297

Table 8. Lowest-Lying Rovibrational Energy Levels of HO_2 for Total Angular Momentum $J = 50$, with Odd Permutation Symmetry and Odd Parity[a]

n	K	Smith/LSFD	this work
1	0	0.346874	0.3469657
2	1	0.349929	0.3500197
3	2	0.363344	0.3634372
4	3	0.379251	0.3793441
5	4	0.400258	0.4003535
6	5	0.425905	0.4260027
7	6	0.456121	0.4562208
8	7	0.471153	0.4712573
9	0	0.474154	0.4742577
10	1	0.487383	0.4874881
11	2	0.490829	0.4909319
12	8	0.503052	0.5031584
13	3		0.5100281
14	0		0.5129769
15	1		0.5238724
16	4		0.5271237
17	2		0.5300602
18	3		0.5435117
19	5		0.5491461
20	9		0.5652686
21	4		0.5735251
22	6		0.5789117
23	5		0.5909422
24	10		0.5918373
25	6		0.5939130
26	7		0.6069630
27	0		0.6130795
28	1		0.6212435
29	2		0.6224414
30	3		0.6231530

[a]All energies are in eV and relative to the vibrational ground state. Previous results from Smith et al.[37] are also presented. New energies are converged to 10^{-6} eV or better; they agree with ref 37 to within 10^{-4} eV or better. Column II: our K assignments (agree with ref 37).

Indeed, one *very* curious trend is the convergence of the $n = 1$ and 2 energy levels with increasing J, leading to the increasingly kinked behavior evident on the left side of Figure 1 (and elsewhere). From the tables, the even-parity, $J = 10$, $n = 1 \rightarrow 2$ level spacing is 0.0022 eV—on the order of the rotational K-level spacing, which is appropriate given the respective K assignments of 0 and 1. As J increases however, the two lowest-lying energies converge exponentially quickly, so that by $J = 120$, they are only about 10^{-6} eV apart! Obviously, the K labels are no longer so suitable for purposes of J-shifting; but the more relevant point here is to try to establish the underlying dynamical cause of this behavior. This is still not settled—although the bound state analog of a bend-rotation Feshbach resonance is suspected (in the same manner that double-well tunneling splitting might be regarded as the bound state analogue of a shape resonance). Section IV C has additional discussion.

We will present a detailed, comprehensive analysis in an upcoming dedicated paper. Here, we restrict ourselves to some preliminary J-shifting results, obtained for just the even-parity rovibrational states for $J = 50$. As a practical measure, application of J-shifting requires some means of assigning K values to those rovibrational states that are being considered, despite possible HC breakdown. In ref 50, the individual K components of the computed bound rovibrational eigenstate wave functions with $J \leq 10$ were consulted, in order to determine the most probable K value (and also vibrational state assignments). Such an approach is not likely feasible for the larger J values, however. Instead, we adopt the following procedure. First, all of the RSD J-shifting rovibrational energies are computed, as per Section II C, and energetically ordered. These are compared to the exact $J = 50$ eigenenergies (energy-ordered, labeled by n), as in Figure 1, and found to match quite closely—apart from being systematically too large by about 1.2×10^{-3} eV. Methods exist for computing accurate rovibrational ground state energies for any J value, that use much less computation than would be required for excited states—for example, Monte Carlo methods. This justifies introducing a systematic energy shift into the RSD J-shifting predictions, so as to make the ground state prediction exact. In any event, RSD energetic ordering as described above leads to unambiguous rotational and vibrational assignments for each of the exact rovibrational states. This procedure is followed throughout this paper, leading to the K and v values as presented in Tables 3−8. These assignments are in perfect agreement with those of ref 50 and of Smith, for the low-lying states for which Smith and co-workers have performed calculations. The higher-lying $J = 10$ state labels also agree with those of ref 50—except for the even-parity $n = 25$ and $n = 26$ K labels, which are switched.

In Table 7, both VSD J-shifting and RSD J-shifting results are presented for the $J = 50$ even-parity states. RSD values are obtained as described above and compared to the exact rovibrational energy levels as computed in this work. For the lowest-lying $n \leq 15$ states, for which exact results are provided in ref 37, those results are used to compare with VSD predictions, also obtained from ref 37. For $n > 15$, we have extrapolated the VSD predictions using the recipe and VSD rotor data from ref 37 (no $v = 3$ data was provided, which is why states $n = 27-30$ are still missing); however, the errors are compared against the exact results from this work. Being customized for individual vibrational states, the VSD scheme is intended to provide more accurate predictions for vibrationally excited rovibrational states than a non-VSD scheme. At such a high J value, however, we find that in fact, *VSD does a fairly poor job for the vibrationally excited states*, even with just a single vibrational excitation, as indicated by the bold-faced entries in the table. In contrast, RSD J-shifting is remarkably consistent and accurate throughout, with most errors just a few meV. A comparison of VSD vs RSD errors for this calculation is presented in graphical form in Figure 2. To enable a fair comparison, the ground-state-energy shift procedure described above for RSD, is here also applied to VSD. Whereas the predictions of the two J-shifting procedures are quite close when there are no vibrational excitations, in general, the VSD errors are an order of magnitude or so worse than those of RSD.

It thus appears that RSD J-shifting can indeed predict the bound rovibrational states of HO_2 quite successfully, even at considerably large J—provided that v and K values are fairly small. Moreover, RSD outperforms VSD, *especially* when there are vibrational excitations.

C.. Wave Function Analysis of a $J = 120$ Rovibrational Bound State. The reason for RSD's success may be understood in terms of eq 10 and the role of centrifugal distortion. As total angular momentum is increased, the minimum geometry of V_{JK}^{eff} is distorted, away from that of V

dx.doi.org/10.1021/jp401154m | J. Phys. Chem. A 2013, 117, 7280−7297

Table 9. Lowest-Lying 125 Rovibrational Energy Levels of HO_2 for Total Angular Momentum $J = 50$, with Odd Permutation Symmetry and Even Parity[a]

n	energy	n	energy	n	energy	n	energy	n	energy
1	0.3377239	26	0.5819257	51	0.6972612	76	0.7771876	101	0.8255161
2	0.3380129	27	0.5822055	52	0.6978582	77	0.7773717	102	0.8321959
3	0.3535472	28	0.5918391	53	0.6981385	78	0.7777674	103	0.8323362
4	0.3629127	29	0.5973373	54	0.6982265	79	0.7786029	104	0.8345098
5	0.3793755	30	0.6064520	55	0.6998362	80	0.7827856	105	0.8391353
6	0.4003546	31	0.6130744	56	0.7130283	81	0.7833484	106	0.8439770
7	0.4260047	32	0.6212383	57	0.7138427	82	0.7857187	107	0.8448200
8	0.4562228	33	0.6224480	58	0.7210979	83	0.7888526	108	0.8452965
9	0.4621111	34	0.6231479	59	0.7220653	84	0.7910431	109	0.8500331
10	0.4623934	35	0.6238717	60	0.7290518	85	0.7944307	110	0.8500982
11	0.4777465	36	0.6241375	61	0.7310211	86	0.7953825	111	0.8514417
12	0.4869664	37	0.6408178	62	0.7378960	87	0.7954248	112	0.8528856
13	0.4909338	38	0.6429098	63	0.7407083	88	0.8022355	113	0.8564731
14	0.4999147	39	0.6499652	64	0.7433171	89	0.8027719	114	0.8587294
15	0.5001664	40	0.6515416	65	0.7435628	90	0.8050560	115	0.8591698
16	0.5032023	41	0.6522968	66	0.7438783	91	0.8066598	116	0.8594119
17	0.5170171	42	0.6524324	67	0.7452464	92	0.8105873	117	0.8621204
18	0.5238741	43	0.6591535	68	0.7494155	93	0.8108701	118	0.8667870
19	0.5264781	44	0.6668068	69	0.7537549	94	0.8111544	119	0.8681210
20	0.5300623	45	0.6678602	70	0.7539767	95	0.8119071	120	0.8700097
21	0.5435514	46	0.6705960	71	0.7580703	96	0.8145130	121	0.8704280
22	0.5491468	47	0.6731157	72	0.7601341	97	0.8156824	122	0.8757258
23	0.5652690	48	0.6803139	73	0.7690520	98	0.8220822	123	0.8760311
24	0.5735271	49	0.6880384	74	0.7691344	99	0.8222201	124	0.8786040
25	0.5789125	50	0.6941553	75	0.7700454	100	0.8226380	125	0.8788423

[a]All energies are in eV and relative to the vibrational ground state. Energies are converged to 10^{-6} eV or better.

itself. For small K, most of this distortion is along the O−O bond—but the heaviness of the atoms limits the extent of this distortion, even for large J values. On the other hand, the K dependence of eq 10 is much more pronounced, owing to the lightness of the H atom—that is, to the fact that $\mu_R \ll \mu_r$ (Table 1). Consequently, V_{JK}^{eff} changes much more dramatically as K is increased, with the H atom pushed substantially outward from O_2. Of course, this has a marked impact on the rotational constants and on the associated RSD J-shifting levels.

The ramifications become quite interesting in the large-J and -K limit. Because the J contribution in eq 10 is large for large J, the V_{JK}^{eff} potential well is greatly diminished by the J contribution alone—that is, even for $K = 0$. At some point—that is, beyond some K value—the K contribution to V_{JK}^{eff} first pushes the potential well above the dissociation threshold and then obliterates it completely, leading in both cases to a scattering potential. This situation—well presaged by Bowman's comment at the start of Section IV B—implies that exact quantum dynamical treatment of the *bound* rovibrational states for the largest J values may actually provide some insight into the *scattering* process. In any event, use of the global minimum in RSD J-shifting would, for the larger K values, lead to completely dissociated H + O_2 as the appropriate geometry—with the H atom infinitely far away from the O_2 diatomic, and $\theta = \pi/2$ (from eq 10). Note that this is the "oblate top" realm, with smaller K values corresponding to more O_2 rotation, and therefore *larger* rotational kinetic energy values. The intriguing prospect of observing mixed prolate and oblate behavior within the K expansion for a *single* quantum dynamical state is not something that has been previously considered, to the authors' best knowledge.

To explore the above scenario, we have performed an accurate quantum dynamical calculation of the even-parity, $J = 120$, $n = 1$ rovibrational eigenstate *wave function*, using the ***ScalIT*** codes. The most telling information to extract from this wave function is the distribution of probability across K values—that is, $\sum_{v_1,v_2,j}|C_{v_1,v_2,j,K}^{J0\varepsilon}|^2$ as a function of K (with $C_{v_1,v_2,j,K}^{JM\varepsilon}$ from eq 4). The results, presented in Figure 3a, exhibit a curious, alternating-K structure, up to about $K = 38$. Beyond this point, there is no oscillation; the probability values simply peter out—steadily but gradually—with increasing K. It is thus abundantly clear that even for just this lowest-lying $n = 1$ eigenstate, even modest K truncation will be ineffective, insofar as accurate rovibrational level calculations are concerned.

More dynamically intriguing, however, is understanding the "$K = 38$ divide." It turns out that this is the crossover point above which the binding-plus-rotation energy for the bound molecule geometry exceeds the O_2 diatomic rotation energy for the H + O_2 dissociated molecule—as demonstrated in Figure 4, a plot of the rotational energy shifts, E_{JK}^{rot} as a function of K, for $J = 120$. Two different curves are presented: one corresponding to the bound molecule local minimum of V_{JK}^{eff}, the other to the dissociated H + O_2 fragments. Due to their respective prolate/oblate natures, as discussed above, the first curve necessarily increases with K, whereas the second necessarily decreases. There is thus an energetic crossover that occurs at some intermediate K value—which from the figure is found to be *exactly* at $K = 38$. Thus, the steady decay evident in Figure 3a for $K > 38$ can be regarded as a tunneling contribution from dissociated configurations that are classically forbidden.

Conversely, the oscillatory behavior observed in the "classical" $K \leq 38$ region must reflect some sort of quantum interference effect. Intuition suggests that this is somehow

dx.doi.org/10.1021/jp401154m | J. Phys. Chem. A 2013, 117, 7280−7297

Table 10. Lowest-Lying Rovibrational Energy Levels of HO_2 for Total Angular Momentum J = 60, 70, and 80, with Odd Permutation Symmetry and Both Even and Odd Parity[a]

index	J = 60		J = 70		J = 80	
n	even	odd	even	odd	even	odd
1	0.4814901	0.4936133	0.6491905	0.6641582	0.8399739	0.8575764
2	0.4816210	0.4955593	0.6492474	0.6652779	0.8399982	0.8581734
3	0.5015303	0.5106492	0.6741319	0.6829679	0.8701106	0.8793496
4	0.5092875	0.5257061	0.6801388	0.6966951	0.8744290	0.8913221
5	0.5258254	0.5464917	0.6970475	0.7172339	0.8921998	0.9116478
6	0.5464906	0.5718998	0.7172134	0.7423246	0.9115790	0.9363206
7	0.5719037	0.6018736	0.7423253	0.7719934	0.9363237	0.9656150
8	0.6018772	0.6144506	0.7661060	0.7808957	0.9521959	0.9695828
9	0.6024624	0.6163612	0.7661615	0.7819958	0.9522198	0.9701711
10	0.6025900	0.6312379	0.7719935	0.7994293	0.9656160	0.9910254
11	0.6222570	0.6363225	0.7907274	0.8061200	0.9819284	0.9993508
12	0.6298900	0.6460665	0.7966403	0.8129509	0.9861872	1.0028352
13	0.6363262	0.6574325	0.8061204	0.8287395	0.9993517	1.0226638
14	0.6441957	0.6592238	0.8124394	0.8296911	1.0035137	1.0229220
15	0.6442852	0.6665640	0.8124645	0.8332291	1.0038461	1.0236190
16	0.6462110	0.6751653	0.8133694	0.8446148	1.0040481	1.0374275
17	0.6659037	0.6753307	0.8331609	0.8488220	1.0227965	1.0463220
18	0.6666606	0.6906816	0.8397022	0.8579384	1.0367250	1.0473855
19	0.6736728	0.6916002	0.8446149	0.8626050	1.0374280	1.0582383
20	0.6751689	0.7121553	0.8454300	0.8837607	1.0406569	1.0760558
21	0.6908349	0.7183141	0.8579370	0.8870374	1.0472392	1.0779360
22	0.6916033	0.7211293	0.8630625	0.8875252	1.0593684	1.0785207
23	0.7121529	0.7309068	0.8789902	0.8935658	1.0607997	1.0791489
24	0.7183178	0.7328030	0.8790462	0.8946616	1.0608236	1.0797983
25	0.7190904	0.7384012	0.8837347	0.9095891	1.0760602	1.0990233
26	0.7192172	0.7474613	0.8870382	0.9118186	1.0790452	1.1044271
27	0.7211319	0.7550529	0.8875256	0.9207957	1.0797976	1.1093425
28	0.7384048	0.7621142	0.9032323	0.9251951	1.0900649	1.1107478
29	0.7385900	0.7656972	0.9090944	0.9343571	1.0943068	1.1262282
30	0.7461439	0.7693726	0.9095954	0.9401463	1.1044314	1.1304655

[a]All energies are in eV and relative to the vibrational ground state. Energies are converged to 10^{-6} eV or better.

related to the fact that the n = 1 and n = 2 eigenenergies are nearly identical (Sec. IV B). Indeed, Figure 3b, depicting the K distribution of probability for the n = 2 state, exhibits remarkable similarity to Figure 3a—except that the oscillations are *exactly complementary*. This is demonstrated in Figure 3c, in which the n = 1 and n = 2 distributions are summed, and the K oscillations are seen to disappear completely. In any event, whether our Feshbach-like-resonance hypothesis is correct or not, from the figure, there can be no doubt that Coriolis coupling is directly involved.

As alluded to above, the crossover point should also provide some useful information about HO_2 reactivity. In particular, for highly rotationally excited HO_2 with $J \geq 38$, we expect to see a decrease in reactivity, owing to the rotational barrier that the fragments must overcome in order to get close enough to react. In Figure 1 of ref 46—even accounting properly for the rotational shift—one does indeed observe a substantial decrease in the cumulative reaction probability for $J > 30$.

As a final validation of the "effective potential" idea, we have created various wave function plots as a function (r, R, θ), for the even-parity, J = 120, n = 1 rovibrational eigenstate, evaluated at two different values of K. Being the lowest-lying eigenstate, the plots all exhibit a single narrow peak, and are otherwise "boring," and not presented. Instead, we focus here on the geometry of maximum probability density for each K value. For K = 0, this geometry occurs at r_{max} = 2.76 au and R_{max} = 2.43 au As per earlier arguments, one expects the majority of the centrifugal distortion for K = 0 to manifest as a modest elongation of the O−O bond. Given that r_{max} = 2.51 au for the vibrational ground state, this is indeed observed to be the case. We have also analyzed the K = 47 component—lying well within the "oblate" region, and for which V_{JK}^{eff} is in fact completely repulsive. An HC calculation would predict only scattering contributions at this K value and significant probability density across an extended R range. In reality, the K = 47 component of the n = 1 eigenstate—like that for K = 0—is found to be narrowly peaked about its R_{max} value. However, R_{max} = 2.51 au is now elongated in comparison to the K = 0 value, and r_{max} = 2.51 is now reduced to its undistorted value—both of which are consistent with a transfer of angular momentum from the body-fixed x and y components to the z component, as might be predicted from eq 10.

V. SUMMARY AND CONCLUDING REMARKS

The HO_2 radical continues to garner much attention in the literature. From previous work, it is clear that the rovibrationally excited states—particularly at very large J—are dynamically very important. Yet, a comprehensive calculation of the bound rovibrational eigenstates of HO_2, up to the highest allowable J values, has never been achieved before now. Specifically, quantum dynamics calculations were performed here for all multiple-of-ten J values in the range $10 \leq J \leq 130$. These

dx.doi.org/10.1021/jp401154m | J. Phys. Chem. A 2013, 117, 7280−7297

Table 11. Lowest-Lying Rovibrational Energy Levels of HO_2 for Total Angular Momentum J = 90, 100, 110, and 120, with Odd Permutation Symmetry and Both Even and Odd Parity[a]

index	J = 90		J = 100		J = 110		J = 120	
n	even	odd	even	odd	even	odd	even	odd
1	1.0527646	1.0727613	1.2862321	1.3083913	1.5387803	1.5628593	1.8084129	1.8341889
2	1.0527750	1.0730654	1.2862365	1.3085427	1.5387826	1.5629348	1.8084138	1.8342270
3	1.0880158	1.0983892	1.3262269	1.3383553	1.5829690	1.5972234	1.8562077	1.8726571
4	1.0908934	1.1083506	1.3280212	1.3462515	1.5840391	1.6031913	1.8568321	1.8769781
5	1.1101888	1.1285859	1.3495601	1.3666311	1.6084220	1.6240569	1.8844073	1.8987298
6	1.1283943	1.1527028	1.3661755	1.3900006	1.6231154	1.6464247	1.8964023	1.9196835
7	1.1527130	1.1794281	1.3872855	1.4091834	1.6335515	1.6573621	1.8966446	1.9221974
8	1.1596826	1.1797273	1.3872942	1.4093334	1.6335582	1.6574344	1.8972683	1.9223523
9	1.1596930	1.1815609	1.3900444	1.4183248	1.6465263	1.6741444	1.9200244	1.9468522
10	1.1815473	1.2046520	1.4183070	1.4386491	1.6740571	1.6911311	1.9437080	1.9599986
11	1.1944483	1.2144154	1.4267433	1.4464852	1.6772137	1.6971176	1.9444647	1.9644190
12	1.1972987	1.2149107	1.4285334	1.4510575	1.6782649	1.7062219	1.9470934	1.9781496
13	1.2148005	1.2344250	1.4496297	1.4665997	1.7021305	1.7177424	1.9715151	1.9859772
14	1.2162542	1.2388514	1.4510834	1.4751764	1.7043515	1.7302425	1.9739670	2.0016423
15	1.2172381	1.2391300	1.4512666	1.4753157	1.7043870	1.7303236	1.9740194	2.0017539
16	1.2173111	1.2523802	1.4513134	1.4877921	1.7062253	1.7395368	1.9780858	2.0065244
17	1.2342732	1.2582805	1.4661834	1.4899774	1.7168718	1.7429449	1.9840017	2.0096983
18	1.2523765	1.2668447	1.4859224	1.5074832	1.7267415	1.7502299	1.9844189	2.0098412
19	1.2555899	1.2762927	1.4859354	1.5075924	1.7267532	1.7503042	1.9848819	2.0141350
20	1.2576888	1.2829851	1.4877945	1.5081100	1.7396041	1.7671933	2.0067433	
21	1.2587155	1.2832858	1.4899775	1.5151020	1.7429516	1.7678282	2.0141272	
22	1.2635146	1.2867260	1.4946360	1.5177889	1.7520550	1.7731301		
23	1.2635259	1.2942385	1.4961654	1.5292689	1.7529209	1.7830725		
24	1.2786318	1.2971337	1.5174676	1.5361674	1.7670906	1.7833539		
25	1.2867171	1.3077577	1.5195195	1.5365266	1.7697871	1.7893109		
26	1.2942356	1.3175297	1.5247792	1.5443134	1.7708253	1.7948157		
27	1.2968395	1.3196106	1.5266016	1.5500856	1.7795370	1.7992365		
28	1.2977552	1.3217059	1.5292687	1.5598208	1.7830772	1.8096838		
29	1.3005963	1.3372550	1.5356406	1.5642454	1.7930621	1.8172147		
30	1.3191352	1.3400808	1.5473471	1.5743792	1.7945925	1.8239492		

[a]All energies are in eV and relative to the vibrational ground state. Energies are converged to 10^{-6} eV or better.

calculations are "exact," in the sense that no K truncation or other approximations to the rovibrational quantum Hamiltonian of eq 2 were applied. For each J value considered, both the even and odd parity states were computed (although the even-permutation-symmetry states are not physically allowed and are therefore ignored).

All calculations were performed using the DMBE IV PES and the ***ScalIT*** suite of parallel codes. DMBE IV is an older PES, not likely very accurate at higher energies. However, it has served as a standard benchmark for other HO_2 bound rovibrational state calculations—which, to the authors' best knowledge, have only previously been performed up to J = 50.[37] For the high convergence accuracies achieved in this study—that is, 10^{-6} eV or better for all computed energy levels—there can be no doubt that the "accuracy bottleneck" of the overall calculation is the DMBE IV PES. Future work may see similar calculations applied to more accurate HO_2 PESs, such as "XXZLG"[41] or one of its variants. From a computational standpoint, all indications are that such calculations would be *less* challenging than those performed here, owing to the reduced density of states (DOS).[38,49] Note also that previous DOS work has focused on the vibrational rather than the rovibrational DOS, yet it is the latter that is of greater practical importance. Accordingly, we may also perform our own rovibrational DOS study in future.

For purposes of addressing the efficacy of the ***ScalIT*** parallel quantum dynamics codes as applied to triatomic molecules at very large J, use of the DMBE IV PES is entirely justified. The fact that we were able to effectively parallelize even a comparatively "small" (from a massively parallel standpoint) problem such as J = 120 HO_2 across one hundred *nodes* (12 cores each) is highly encouraging—although this did involve a bit of "tweaking" and exposed some unexpected issues. On the other hand, running across a more modest five nodes (60 cores) presented no special consideration or difficulties whatsoever and resulted in typical MPI wall times well under one hour per job. Moreover, it must be emphasized that all ***ScalIT*** jobs were executed here in the manner of a "non-expert" user—that is, by using only default algorithms and high-level modules, and paying little explicit attention to optimization. Almost anyone—following the "recipe" described in the Supporting Information, and provided with access to a modest-sized cluster—could have duplicated the results obtained here. Together with ref 50, this work is thus intended to demonstrate the viability and robustness of ***ScalIT*** as an effective computational tool for nonexpert users from the general chemical dynamics field—as opposed, for example, to various previous numerically oriented investigations.[60−63]

At the same time, HO_2 also serves as an ideal testbed for parallel quantum dynamics methodologies, because: (a) many previous studies are available in the literature; (b) such

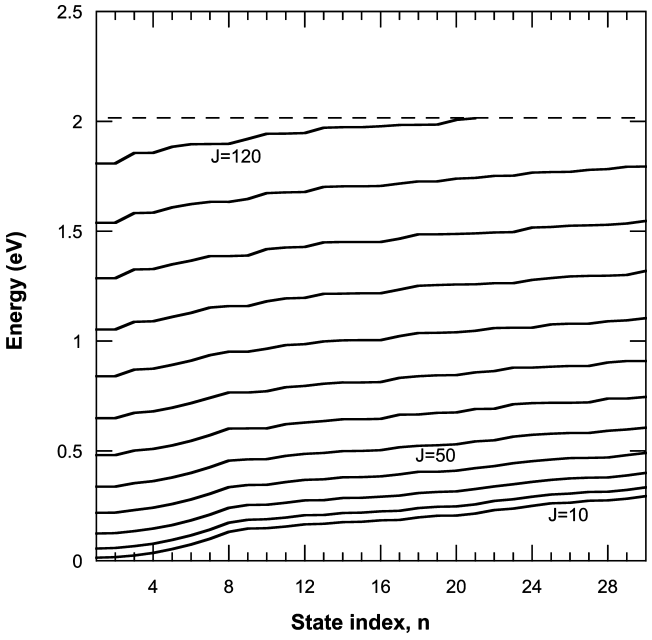

Figure 1. Lowest-lying 30 even-parity rovibrational energy levels of HO_2, as a function of state index n, for each multiple-of-ten value of total angular momentum J, from J = 10−120. All energies are in eV and relative to the vibrational ground state. The different J curves resemble each other, apart from an energy shift. The dashed line represents the dissociation threshold.

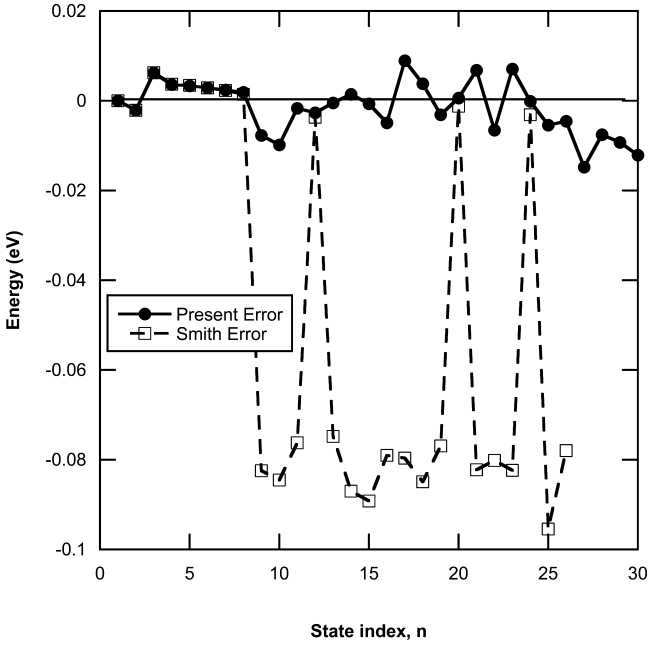

Figure 2. Error comparison for VSD (Smith) vs RSD (our) J-shifting, for the lowest-lying 30 rovibrational energy levels of HO_2, for total angular momentum J = 50, with odd permutation symmetry and even parity, as a function of state index n. For accurate comparison, ground-state-energy shifting has been applied to both predictions (i.e., the error for the n = 1 state is zero). This convention differs from the VSD results as presented in Table 7 and in ref 37.

calculations, especially for the rovibrational states, are still considered extremely challenging; (c) certain dynamical features such as HC breakdown are still poorly understood; (d) other parallel methods have been applied to this system.

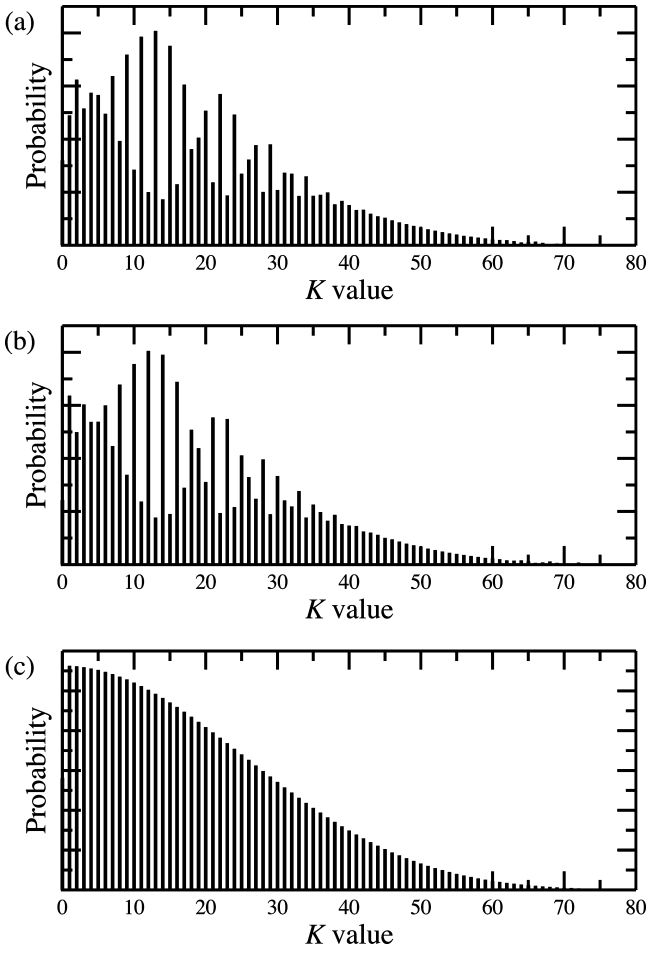

Figure 3. Distribution of probability across K, for lowest-lying rovibrational eigenstate wave functions of HO_2, for total angular momentum J = 120, with odd permutation symmetry and even parity: (a) n = 1 eigenstate; (b) n = 2 eigenstate; (c) sum of n = 1 and n = 2.

Whereas ref 50 focused more on (d), in this paper, it is (c) that has been primarily emphasized. Given that the J-shifting and HC approximations are *theoretical* models, it is our view that any honest assessment of these techniques requires comparison with exact rovibrational spectroscopy calculations performed using the same PES—rather than, say, via comparison with experiment. We have endeavored to provide just such an assessment here, at least for our RSD J-shifting method (in which context, also, the use of the DMBE IV PES is entirely justified). In contrast, the VSD J-shifting predictions rely on experimental VSD rotational constants, which may indeed help to explain why this approach behaves so poorly when applied at very large J values—that is, well outside the range of the experimental fitting parameters.

On the other hand, it is *precisely* the large-J regime that presents the greatest topical interest—and computational challenges—for the HO_2 system. In this paper, we confirm the conclusion reached by many previous researchers, that HO_2 at large J experiences *severe* Coriolis coupling and HC breakdown. For this reason (and also because the HC approximation is embedding-dependent), we did not deem it fruitful to perform any HC calculations here. Yet remarkably, Figure 1 indicates that the vibrationally low-lying rovibrational energy levels are indeed characterized by some sort of J-shifting, across the entire J range. Moreover our particular RSD J-

dx.doi.org/10.1021/jp401154m | J. Phys. Chem. A 2013, 117, 7280−7297

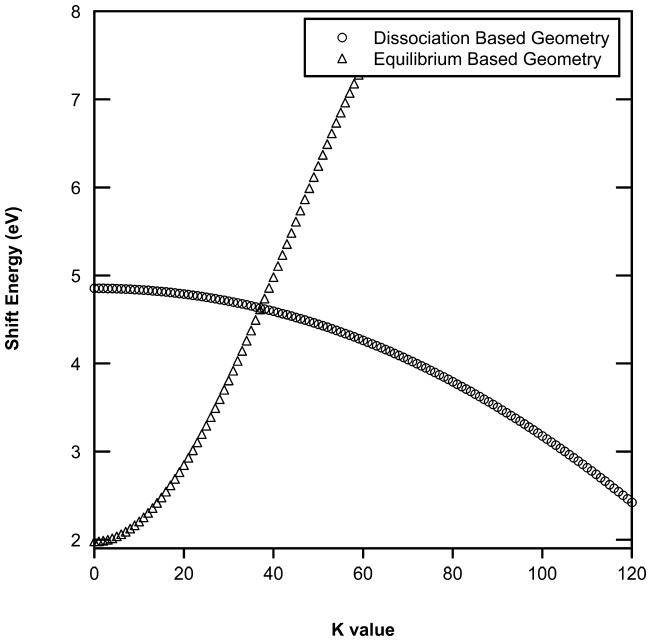

Figure 4. RSD rotational energy shifts, E_{JK}^{rot}, as a function of K, for J = 120, as computed using the method of Section II C applied to the DMBE IV PES. Triangles correspond to local V_{JK}^{eff} minimum geometry associated with the bound HO_2 molecule. Circles correspond to the dissociated H + O_2 fragments. There is an energetic crossover between the two curves at K = 38.

shifting scheme is found to yield surprisingly accurate predictions for the rotational energy shifts, even for considerably large J. We deem this to be a sufficiently important finding as to justify a whole other article addressing this theme alone.

The underlying dynamical picture upon which RSD J-shifting is based—that is, that of the three-body "effective potential," consisting of the true potential plus a centrifugal correction, in exact analogy with the familiar two-body case—is further found to provide additional benefits. In particular, this description yields important dynamical insight into the K-structure of the exact quantum dynamical rovibrational eigenstate wave functions, even at the very highest J = 120 value for which such states are (now) known to exist. Almost unused since its invention in 1998,[56,57,85] despite exhibiting substantial promise, the three-body effective potential idea—conceptually simple, yet practically useful—will, it is to be hoped, be adopted by other researchers, going forward.

It is also to be hoped that the utility, efficiency, and ease-of-use of ***ScalIT***—as have by now been amply demonstrated[50,60−64,82,83]—will also attract converts, going forward. These might include nonexperts such as experimentalists, who have a practical need to compute accurate rovibrational state data reliably and quickly, as well as the more "expert" quantum dynamics practitioner, with the desire to introduce massively parallel functionality into his or her existing code base. For either type of user, both the ***ScalIT*** package itself, and the associated documentation, will be made available from the authors on request.

■ ASSOCIATED CONTENT

Ⓢ Supporting Information

A practical, step-by-step user's guide, to enable the nonexpert ***ScalIT*** user to get up to speed with these codes as quickly as possible. This material is available free of charge via the Internet at http://pubs.acs.org.

■ AUTHOR INFORMATION

Corresponding Author

*Phone: 806-742-3099; e-mail: bill.poirier@ttu.edu.

Notes

The authors declare no competing financial interest.

■ ACKNOWLEDGMENTS

This work was largely supported by both a research grant (CHE-1012662) and a CRIF MU instrumentation grant (CHE-0840493) from the National Science Foundation. Additional support from The Robert A. Welch Foundation (D-1523) is also acknowledged, as well as from the Office of Advanced Scientific Computing Research, Mathematical, Information, and Computational Sciences Division of the US Department of Energy under contract DE-FG03-02ER25534. We also gratefully acknowledge the following entities for providing access and technical support for their respective computing clusters: the Texas Tech University High Performance Computing Center, for use of the Hrothgar facility; NSF CHE-0840493 and the Texas Tech University Department of Chemistry and Biochemistry, for use of the Robinson cluster; Carlos Rosales-Fernandez and the Texas Advanced Computing Center, for use of the Lonestar facility. Calculations presented in this paper were performed using the ***ScalIT*** suite of parallel codes.

■ REFERENCES

(1) Du, H.; Hessler, J. P. Rate Coefficient for the Reaction H + O_2 → OH + O: Results at high temperatures, 2000 to 5300 K. *J. Chem. Phys.* **1992**, *96*, 1077−1092.

(2) Yang, H.; Gardiner, W. C.; Shin, K. S.; Fujii, N. Shock Tube Study of the Rate Coefficient of H + O_2→ OH + O. *Chem. Phys. Lett.* **1994**, *231*, 449−453.

(3) Honma, K. Laser Initiated Half Reaction Study of H + O_2→ OH + O. *J. Chem. Phys.* **1995**, *102*, 7856−7863.

(4) Fink, E. H.; Ramsay, D. A. High-Resolution Study of the $\tilde{A}^2A' \rightarrow \tilde{X}^2A''$ Transition of HO_2: Analysis of the 000−000 band. *J. Mol. Spectrosc.* **1997**, *185*, 304−324.

(5) Fink, E. H.; Ramsay, D. A. High-Resolution Study of the $\tilde{A}^2A' \rightarrow \tilde{X}^2A''$ Transition of DO_2: Analysis of the 000−000 band. *J. Mol. Spectrosc.* **2002**, *216*, 322−334.

(6) Anglada, J. M.; Olivella, S.; Sole, S. Mechanistic Study of the $CH_3O_2^{\bullet}$ + $HO_2^{\bullet}$ → CH_3O_2H + O_2 Reaction in the Gas Phase. Computational evidence for the formation of a hydrogen-bonded diradical complex. *J. Phys. Chem. A* **2006**, *110*, 6073−6082.

(7) Thiebaud, J.; Crunaire, S.; Fittschen, C. Measurements of Line Strengths in the $2\nu_1$ Band of the HO_2 Radical Using Laser Photolysis/Continuous Wave Cavity Ring-Down Spectroscopy (cw-CRDS). *J. Phys. Chem. A* **2007**, *111*, 6859−6966.

(8) Melius, C. F.; Blint, R. J. The Potential Energy Surface of the HO_2 Molecular System. *Chem. Phys. Lett.* **1979**, *64*, 183−189.

(9) Pastrana, M. R.; Quintales, L. A. M.; Brandao, J.; Varandas, A. J. C. Recalibration of a Single-valued Double Many-body Expansion Potential Energy Surface for Ground-state Hydroperoxy and Dynamics Calculations for the oxygen atom + hydroxyl → oxygen + hydrogen atom Reaction. *J. Phys. Chem.* **1990**, *94*, 8073−8080.

(10) Leforestier, C.; Miller, W. H. Quantum Mechanical Calculation of the Rate Constant for the Reaction H + O_2 → OH + O. *J. Chem. Phys.* **1994**, *100*, 733−735.

(11) Zhang, D. H.; Zhang, J. Z. H. Quantum Reactive Scattering with a Deep Well: Time-dependent calculation for H+O_2 reaction and bound state characterization for HO_2. *J. Chem. Phys.* **1994**, *101*, 3671−3678.

(12) Dai, J.; Zhang, J. Z. H. Time-dependent Spectral Calculation of Bound and Resonance Energies of HO_2. *J. Chem. Phys.* **1996**, *104*, 3664−3671.
(13) Qi, J.; Bowman, J. M. The Effect of Rotation on Resonances: Application to HCO. *J. Chem. Phys.* **1996**, *105*, 9884−9889.
(14) Kendrick, B.; Pack, R. T. Recombination Resonances in Thermal H + O_2 Scattering. *Chem. Phys. Lett.* **1995**, *235*, 291−296.
(15) Kendrick, B.; Pack, R. T. Potential Energy Surfaces for the Low-Lying $^2A''$ and $^2A'$ States of HO_2: Use of the diatomics in molecules model to fit ab initio data. *J. Chem. Phys.* **1995**, *102*, 1994−2012.
(16) Kendrick, B.; Pack, R. T. Geometric Phase Effects in H + O_2 Scattering. II. Recombination resonances and state-to-state transition probabilities at thermal energies. *J. Chem. Phys.* **1996**, *104*, 7502−7514.
(17) Kendrick, B.; Pack, R. T. Geometric Phase Effects in the Resonance Spectrum, State-to-state Transition Probabilities and Bound State Spectrum of HO_2. *J. Chem. Phys.* **1997**, *106*, 3519−3539.
(18) Quéméner, G.; Balakrishnan, N.; Kendrick, B. K. Quantum Dynamics of the O + OH → H + O_2 Reaction at Low Temperatures. *J. Chem. Phys.* **2008**, *129*, 224309.
(19) Quéméner, G.; Kendrick, B. K.; Balakrishnan, N. Quantum Dynamics of the H + O_2 → O + OH Reaction. *J. Chem. Phys.* **2010**, *132*, 014302.
(20) Pack, R. T.; Butcher, E. A.; Parker, G. A. Accurate Three-Dimensional Quantum Probabilities and Collision Lifetimes of the H + O_2 Combustion Reaction. *J. Chem. Phys.* **1995**, *102*, 5998−6012.
(21) Barclay, V. J.; Dateo, C. E.; Hamilton, I. P.; Kendrick, B.; Pack, R. T. Anomalous Symmetries of the Rovibrational States of HO_2: Consequences of a conical intersection. *J. Chem. Phys.* **1995**, *103*, 3864−3867.
(22) Barclay, V. J.; Hamilton, I. P. Theoretical Study of Fermi Resonance in the Vibrational Spectrum of HO_2. *J. Chem. Phys.* **1995**, *103*, 2834−2838.
(23) Mandelshtam, V. A.; Grozdanov, T. P.; Taylor, H. S. Bound States and Resonances of the Hydroperoxyl Radical HO_2: An accurate quantum mechanical calculation using filter diagonalization. *J. Chem. Phys.* **1995**, *103*, 10074−10084.
(24) Mandelshtam, V. A.; Taylor, H. S.; Miller, W. H. Collisional Recombination Reaction H+O_2+M → HO_2+M: Quantum mechanical study using filter diagonalization. *J. Chem. Phys.* **1996**, *105*, 496−503.
(25) Dobbyn, A. J.; Stumpf, M.; Keller, H.-M.; Schinke, R. Theoretical Study of the Unimolecular Dissociation HO_2→ H+O_2. I. Calculation of the bound states of HO_2 up to the dissociation threshold and their statistical analysis. *J. Chem. Phys.* **1995**, *103*, 9947−9962.
(26) Dobbyn, A. J.; Stumpf, M.; Keller, H.-M.; Hase, W. L.; Schinke, R. Quantum Mechanical Study of the Unimolecular Dissociation of HO_2: A rigorous test of RRKM theory. *J. Chem. Phys.* **1995**, *102*, 5867−5870.
(27) Dobbyn, A. J.; Stumpf, M.; Keller, H.-M.; Schinke, R. Theoretical Study of the Unimolecular Dissociation HO_2→ H+O_2. II. Calculation of resonant states, dissociation rates, and O_2 product state distributions. *J. Chem. Phys.* **1996**, *104*, 8357−8381.
(28) Mahapatra, S. Time Domain Analysis of the Bound States and Resonances of the Hydroperoxy Radical HO_2: Signature of quantum chaos. *J. Chem. Phys.* **1996**, *105*, 344−345.
(29) Wu, X. T.; Hayes, E. F. HO_2 Rovibrational Eigenvalue Studies for Nonzero Angular Momentum. *J. Chem. Phys.* **1997**, *107*, 2705−2719.
(30) Meijer, A. J. H. M.; Goldfield, E. M. Time-Dependent Quantum Mechanical Calculations on H + O_2 for Total Angular Momentum J > 0. *J. Chem. Phys.* **1998**, *108*, 5404−5413.
(31) Meijer, A. J. H. M.; Goldfield, E. M. Time-Dependent Quantum Mechanical Calculations on H + O_2 for Total Angular Momentum J > 0. II: On the importance of Coriolis coupling. *J. Chem. Phys.* **1999**, *110*, 870−880.
(32) Goldfield, E. M.; Meijer, A. J. H. M. Time-dependent Quantum Mechanical Calculations on H + O_2 for Total Angular Momentum J > 0. III. Total cross sections. *J. Chem. Phys.* **2000**, *113*, 11055−11062.
(33) Zhang, H.; Smith, S. C. Calculation of Product State Distributions from Resonance Decay via Lanczos Subspace Filter Diagonalization: Application to HO_2. *J. Chem. Phys.* **2001**, *115*, 5751−5758.
(34) Zhang, H.; Smith, S. C. Calculation of Bound and Resonance States of HO_2 for Nonzero Total Angular Momentum. *J. Chem. Phys.* **2003**, *118*, 10042−10050.
(35) Zhang, H.; Smith, S. C. Converged Quantum Calculations of HO_2 Bound States and Resonances for J = 6 and 10 Rovibrational HO_2. *J. Chem. Phys.* **2004**, *120*, 9583−9593.
(36) Zhang, H.; Smith, S. C. Unimolecular Rovibrational Bound and Resonance States for Large Angular Momentum: J = 20 calculations for HO_2. *J. Chem. Phys.* **2005**, *123*, 014308.
(37) Zhang, H.; Smith, S. C. HO_2 Rovibrational Bound State Calculations for Large Angular Momentum: J = 30, 40, and 50. *J. Phys. Chem. A* **2006**, *110*, 3246−3253.
(38) Zhang, H.; Smith, S. C. Calculation of HO_2 Density of States on Three Potential Energy Surfaces. *J. Theor. Comput. Chem.* **2010**, *9*, 653−665.
(39) Xu, C.; Xie, D.; Zhang, D. H.; Lin, S. Y.; Guo, H. A New ab initio Potential-Energy Surface of $HO_2(X^2A'')$ and Quantum Studies of HO_2 Vibrational Spectrum and Rate Constants for the H+O_2 ↔ O +OH reactions. *J. Chem. Phys.* **2005**, *122*, 244305.
(40) Xu, C.; Xie, D.; Honvault, P.; Lin, S. Y.; Guo, H. Rate Constant for $OH(^2\Pi)$ + $O(^3P)$ → $H(^2S)$ + $O_2(^3\Sigma_g^-)$ Reaction on an Improved ab initio Potential Energy Surface and Implications for the Interstellar Oxygen Problem. *J. Chem. Phys.* **2007**, *127*, 024304.
(41) Xu, C.; Jiang, B.; Xie, D.; Farantos, S. C.; Lin, S. Y.; Guo, H. Analysis of the HO_2 Spectrum on an Accurate ab initio Potential Energy Surface. *J. Phys. Chem. A* **2007**, *111*, 10353−10361.
(42) Xie, D.; Xu, C.; Ho, T.-K.; Rabitz, H. A.; Lendvay, G.; Lin, S. Y.; Guo, H. Global Analytical Potential Energy Surfaces for HO_2 Based on High-level ab initio Calculations. *J. Chem. Phys.* **2007**, *126*, 074315.
(43) Lin, S. Y.; Guo, H.; Honvault, P.; Xu, C.; Xie, D. Accurate Quantum Mechanical Calculations of Differential and Integral Cross Sections and Rate Constant for the O + OH Reaction Using an ab initio Potential Energy Surface. *J. Chem. Phys.* **2008**, *128*, 014303.
(44) Lin, S. Y.; Sun, Z.; Guo, H.; Zhang, D. H.; Honvault, P.; Xie, D.; Lee, S.-Y. Fully Coriolis-Coupled Quantum Studies of the H + O_2 (v_i=0−2,j_i=0,1) → OH + O Reaction on an Accurate Potential Energy Surface: Integral cross sections and rate constants. *J. Phys. Chem. A* **2008**, *112*, 602−611.
(45) Lique, F.; Jorfi, M.; Honvault, P.; Halvick, P.; Lin, S. Y.; Guo, H.; Xie, D. Q.; Dagdigian, P. J.; Klos, J.; Alexander, M. H.; OH, O + → O_2 + H: A Key Reaction for Interstellar Chemistry. New theoretical results and comparison with experiment. *J. Chem. Phys.* **2009**, *131*, 221104.
(46) Ma, J.; Lin, S. Y.; Guo, H.; Sun, Z.; Zhang, D. H.; Xie, D. State-to-State Quantum Dynamics of the $O(^3P)$ + $OH(^2\Pi)$ → $H(^2S)$ + $O_2(^3\Sigma_g^-)$ reaction. *J. Chem. Phys.* **2010**, *133*, 054302.
(47) Sun, Z.; Zhang, D. H.; Xu, C. X.; Zhou, S. L.; Xie, D. Q.; Lendvay, G.; Lee, S.-Y.; Lin, Y.; Guo, H. State-to-State Dynamics of H +O_2 Reaction, Evidence for Non-statistical Behavior. *J. Am. Chem. Soc.* **2008**, *130*, 14962−14963.
(48) Sun, Z.; Lin, X.; Lee, S.-Y.; Zhang, D. H. A Reactant-Coordinate-Based Time-Dependent Wave Packet Method for Triatomic State-to-State Reaction Dynamics: Application to the H +O_2 reaction. *J. Phys. Chem. A* **2009**, *113*, 4145−4154.
(49) Troe, J.; Ushakov, V. G. Anharmonic Rovibrational Numbers and Densities of States for HO_2, H_2CO, and H_2O_2. *J. Phys. Chem. A* **2009**, *113*, 3940−3945.
(50) Chen, W.; Poirier, B. Quantum Dynamical Calculation of All Rovibrational States of HO_2 for Total Angular Momentum J = 0−10. *J. Theor. Comput. Chem.* **2010**, *9*, 435−469.
(51) Barnes, G. L.; Kellman, M. E. Communication: Effective Spectroscopic Hamiltonian for Multiple Minima with Above Barrier Motion: Isomerization in HO_2. *J. Chem. Phys.* **2010**, *133*, 101105.
(52) Miller, J. A.; Kee, R. J.; Westbrook, C. K. Chemical Kinetics and Combustion Modeling. *Annu. Rev. Phys. Chem.* **1990**, *41*, 345−387.

(53) Sun, Q.; Bowman, J. M.; Schatz, G. C.; Sharp, J. R.; Connor, J. N. L. Reduced-Dimensionality Quantum Calculations of the Thermal Rate Coefficient for the CI + HCI → CIH + CI Reaction: Comparison with centrifugal-sudden distorted wave, coupled channel hyperspherlcal, and experimental results. *J. Chem. Phys.* **1990**, *92*, 1677−1686.
(54) Bowman, J. M. Reduced Dimensionality Theory of Quantum Reactive Scattering. *J. Phys. Chem.* **1991**, *95*, 4960−4968.
(55) Bowman, J. M. A Test of an Adiabatic Treament of Rotation for Vibration/Rotation Energies of Polyatomic Molecules. *Chem. Phys. Lett.* **1994**, *217*, 36−40.
(56) Poirier, B. Quantum Reactive Scattering for Three-body Systems via Optimized Preconditioning, as Applied to the O+HCl Reaction. *J. Chem. Phys.* **1998**, *108*, 5216−5224.
(57) Poirier, B. Analytical Treatment of Coriolis Coupling for Three-body Systems. *Chem. Phys.* **2005**, *308*, 305−315.
(58) Pack, R. Space-fixed vs. Body-fixed Axes in Atom-diatomic Molecule Scattering. Sudden approximations. *J. Chem. Phys.* **1974**, *60*, 633−639.
(59) McGuire, P.; Kouri, D. J. Quantum Mechanical Close Coupling Approach to Molecular Collisions. j_z-Conserving Coupled States Approximation. *J. Chem. Phys.* **1974**, *60*, 2488−2499.
(60) Chen, W.; Poirier, B. Parallel Implementation of Efficient Preconditioned Linear Solver for Grid-based Applications in Chemical Physics. I. Block Jacobi Diagonalization. *J. Comput. Phys.* **2006**, *219*, 185−197.
(61) Chen, W.; Poirier, B. Parallel Implementation of Efficient Preconditioned Linear Solver for Grid-based Applications in Chemical Physics. II. QMR Linear Solver. *J. Comput. Phys.* **2006**, *219*, 198−209.
(62) Chen, W.; Poirier, B. Parallel Implementation of Efficient Preconditioned Linear Solver for Grid-based Applications in Chemical Physics: III. Improved Parallel Scalability. *J. Parallel Distrib. Comput.* **2010**, *70*, 779−782.
(63) Chen, W.; Poirier, B. Quantum Dynamics on Massively Parallel Computers: Efficient numerical implementation for preconditioned linear solvers and eigensolvers. *J. Theor. Comput. Chem.* **2010**, *9*, 825−846.
(64) Yang, B.; Chen, W.; Poirier, B. Rovibrational Bound States of Neon Trimer: Quantum dynamical calculation of all eigenstate energy levels and wavefunctions. *J. Chem. Phys.* **2011**, *135*, 094306.
(65) Poirier, B.; Light, J. C. Phase Space Optimization of Quantum Representations: Direct product basis sets. *J. Chem. Phys.* **1999**, *111*, 4869−4885.
(66) Poirier, B.; Light, J. C. Phase Space Optimization of Quantum Representations: Three-body systems, and the bound states of HCO. *J. Chem. Phys.* **2001**, *114*, 6562−6571.
(67) Poirier, B. Phase Space Optimization of Quantum Representations: Non-Cartesian coordinate spaces. *Found. Phys.* **2001**, *31*, 1581−1610.
(68) Bian, W.; Poirier, B. Accurate and Highly Efficient Calculation of the O(^1D)HCl Vibrational Bound States, Using a Combination of Methods. *J. Theo. Comput. Chem.* **2003**, *2*, 583−597.
(69) Huang, S.-W.; Carrington, T., Jr. A New Iterative Method for Calculating Energy Levels and Wave Functions. *J. Chem. Phys.* **2000**, *112*, 8765−8771.
(70) Poirier, B.; Carrington, T., Jr. Accelerating the Calculation of Energy Levels and Wave Functions Using an Efficient Preconditioner with the Inexact Spectral Transform Method. *J. Chem. Phys.* **2001**, *114*, 9254−9264.
(71) Poirier, B.; Carrington, T., Jr. A Preconditioned Inexact Spectral Transform Method for Calculating Resonance Energies and Widths, as Applied to HCO. *J. Chem. Phys.* **2002**, *116*, 1215−1227.
(72) Poirier, B.; Miller, W. H. Optimized Preconditioners for Green Function Evaluation in Quantum Reactive Scattering Calculations. *Chem. Phys. Lett.* **1997**, *265*, 77−83.
(73) Poirier, B. Optimal Separable Bases and Series Expansions. *Phys. Rev. A* **1997**, *56*, 120−130.
(74) Poirier, B. Efficient Preconditioning Scheme for Block Partitioned Matrices with Structured Sparsity. *Numer. Linear Algebra Appl.* **2000**, *7*, 715−726.
(75) Wyatt, R. E. Matrix Spectroscopy: Computation of Interior Eigenstates of Large Matrices Using Layered Iteration. *Phys. Rev. E* **1995**, *51*, 3643−3658.
(76) Goldfield, E. M.; Gray, S. K. Mapping Coriolis-Coupled Quantum Dynamics onto Parallel Computer Architectures. *Comput. Phys. Commun.* **1996**, *98*, 1−14.
(77) Zhang, J. Z. H. *Theory and application of quantum molecular dynamics*; World Scientific, Singapore, 1999.
(78) Mussa, H. Y.; Tennyson, J. Bound and Quasi-Bound Rotation-Vibrational States Using Massively Parallel Computers. *J. Comput. Phys. Commun.* **2000**, *128*, 434−445.
(79) Wang, X.-G.; Carrington, T., Jr. Quantum Dynamics on Massively Parallel Computers: Efficient numerical implementation for preconditioned parallel methods for high-dimensional quantum dynamics. *Comput. Phys. Commun.* **2009**, *181*, 455−461.
(80) Lanczos, C. An Iteration Method for the Solution of the Eigenvalue Problem of Linear Differential and Integral Operators. *J. Res. Natl. Bur. Stand.* **1950**, *45*, 255−282.
(81) Freund, R. W.; Nachtigal, N. M. QMR: A quasi-minimal residual method for non-Hermitian linear systems. *Numer. Math.* **1991**, *60*, 315−339.
(82) Yang, B.; Poirier, B. Quantum Dynamical Calculation of Rovibrational Bound States of Ne_2Ar. *J. Phys. B* **2012**, *45*, 135102.
(83) Yang, B.; Poirier, B. Rovibrational Bound States of the Ar_2Ne Complex. *J. Theor. Comput. Chem.* **2012**, *12*, 1250107.
(84) Burkholder, J. B.; Hammer, P. D.; Howard, C. J.; Towle, J. P.; Brown, J. M. Fourier Transform Spectroscopy of the ν_2 and ν_3 Bands of HO_2. *J. Mol. Spectrosc.* **1992**, *151*, 493−512.
(85) Xiao, Y. S.; Poirier, B. Accurate Quantum Calculation of the Bound and Resonant Rovibrational States of $Li^-(H_2)$. *J. Chem. Phys.* **2005**, *122*, 124318.
(86) Colbert, D. T.; Miller, W. H. A Novel Discrete Variable Representation for Quantum Mechanical Reactive Scattering via the S-matrix Kohn Method. *J. Chem. Phys.* **1992**, *96*, 1982−1990.